Quantitative physiology and biomass composition of *Cyberlindnera jadinii* in ethanol-grown cultures

Marcel A. Vieira-Lara[#], Marieke Warmerdam, Erik A. F. de Hulster, Marcel van den Broek, Jean-Marc Daran, Jack T. Pronk*

Department of Biotechnology, Delft University of Technology, van der Maasweg 9, 2629, HZ Delft, the Netherlands

Corresponding authors:

[#]M.A.VieiraLara@tudelft.nl

*J.T.Pronk@tudelft.nl, tel. +31 15 2782473

Running title: From ethanol to protein with *Cyberlindnera jadinii*

Abstract

Background

Elimination of greenhouse gas emissions in industrial biotechnology requires replacement of carbohydrates by alternative carbon substrates, produced from CO_2 and waste streams. Ethanol is already industrially produced from agricultural residues and waste gas and is miscible with water, self-sterilising and energy-dense. The yeast *C. jadinii* can grow on ethanol and has a history in the production of single-cell protein (SCP) for feed and food applications. To address a knowledge gap in quantitative physiology of *C. jadinii* during growth on ethanol, this study investigates growth kinetics, growth energetics, nutritional requirements, and biomass composition of *C. jadinii* strains in batch, chemostat and fed-batch cultures.

Results

In aerobic, ethanol-limited chemostat cultures, the thiamine-auxotrophic strain *C. jadinii* CBS 621 exhibited a maximum biomass yield on ethanol ($Y_{x/s}^{max}$) of 0.83 $g_{biomass} \cdot (g_{ethanol})^{-1}$ and an estimated maintenance requirement for ATP (m_{ATP}) of 0.28 $mmol \cdot (g_{biomass})^{-1} \cdot h^{-1}$. Even at specific growth rates below 0.05 h^{-1}, a stable protein content of approximately 0.54 $g_{protein} \cdot (g_{biomass})^{-1}$ was observed. At low specific growth rates, up to 17% of the proteome consisted of alcohol dehydrogenase proteins, followed by aldehyde dehydrogenases and acetyl-CoA synthetase. Of 13 *C. jadinii* strains evaluated, 11 displayed fast growth on ethanol ($\mu_{max} > 0.4\ h^{-1}$) in mineral medium without vitamins. The prototrophic strain *C. jadinii* CBS 5947 was grown on an inorganic salts medium in fed-batch cultures fed with pure ethanol. Biomass concentrations in these cultures increased up to 100 $g \cdot L^{-1}$, with a biomass yield of 0.65 $g_{biomass} \cdot (g_{ethanol})^{-1}$. Model-based simulation, based on quantitative parameters determined in chemostat cultures, adequately predicted biomass production. A different protein content of chemostat- and fed-batch-grown biomass (54% and 42%, respectively) may reflect the more dynamic conditions in fed-batch cultures.

43 **Conclusions**

44 Analysis of ethanol-grown batch, chemostat and fed-batch cultures provided a quantitative
45 physiology baseline for fundamental and applied research on *C. jadinii*. Its high maximum growth
46 rate, high energetic efficiency of ethanol dissimilation, simple nutritional requirements and high
47 protein content, make *C. jadinii* a highly interesting platform for production of SCP and other
48 products from ethanol.

49 Keywords (3-10):

50 Ethanol, yeast, *Candida utilis*, protein, physiology, growth rate, chemostat

51

52 **Introduction**

53 Establishing a circular, net-zero emission industrial biotechnology industry requires replacing
54 refined sugars, which are currently the predominant carbon sources for industrial fermentation
55 processes, with feedstocks derived from CO_2 and renewable waste streams (1, 2). Especially for
56 products whose synthesis is ATP intensive, process intensity will benefit from first converting these
57 primary carbon sources into small organic molecules that can be used as substrates to generate the
58 product of interest in separate intensive, aerobic fermentation processes (1). In addition to microbial
59 fermentation of lignocellulosic residues from agriculture and forestry (3), such small molecules can
60 be produced by gas fermentation (4), electrochemical production from CO_2 (1, 5) and, potentially,
61 from microbial electrosynthesis (6, 7). The resulting organic molecules include C_1 compounds such
62 as formic acid and methanol as well as the C_2 compounds acetic acid and ethanol (1).

63 Ethanol is an energy-dense substrate that is completely miscible in water and, at high
64 concentrations, self-sterilising. Especially at low pH, ethanol is less toxic than other C_1 and C_2
65 compounds generated from CO_2. Yeast-based production of ethanol from agricultural residues (8)
66 and production of ethanol from waste gases by engineered strains of *Clostridium autoethanogenum*
67 (4, 9) have both transitioned to industrial scale. Ethanol can be readily assimilated by a variety of
68 microorganisms (10), including yeast species that are already applied in large-scale sugar-based
69 fermentation processes. However, compared to the wealth of information on quantitative physiology
70 of sugar-grown aerobic cultures of industrially relevant yeast species, quantitative information on
71 the stoichiometry, kinetics, and energetics of ethanol-grown cultures of such yeasts is scarce (11).

72 After diffusion over the yeast plasma membrane (12), ethanol is first converted to acetyl-CoA. This
73 conversion involves the enzymes NAD^+-dependent alcohol dehydrogenase, $NAD(P)^+$-dependent
74 acetaldehyde dehydrogenase and acetyl-CoA synthetase. Further dissimilation and assimilation of

75 acetyl-CoA involves the tricarboxylic acid (TCA) cycle, glyoxylate cycle and gluconeogenesis.
76 Dissimilation of ethanol to CO_2 generates reduced cofactors (5 NAD(P)H and 1 $FADH_2$) and requires
77 input of one ATP-equivalent due to the combination of the investment of 2 ATP equivalents in the
78 acetyl-CoA synthetase reaction (13) and the formation of 1 ATP equivalent by substrate-level
79 phosphorylation in the TCA cycle. Energy coupling of the subsequent reoxidation of NADH and
80 $FADH_2$ by mitochondrial respiration has a strong impact on the net ATP yield from ethanol
81 dissimilation and, thereby, on product yields on ethanol and on oxygen. The efficiency of this energy
82 coupling is expressed by the P/O ratio, which indicates how many moles of ATP oxidative
83 phosphorylation generates when a single electron pair (for example derived from NADH) is
84 transferred to oxygen.

85 Involvement of an active multi-subunit proton-pumping NADH dehydrogenase ('Complex I')
86 in the mitochondrial respiratory chains of yeasts strongly influences their P/O ratio (14, 15). Several
87 industrially relevant yeasts, such as *Saccharomyces cerevisiae* and *Kluyveromyces lactis*, lack the
88 genetic information for synthesizing Complex I and, instead, only harbour single-subunit, non-
89 proton-translocating NADH dehydrogenases (16, 17). Other yeasts encode the genetic information
90 for synthesizing both Complex I and non-proton-translocating NADH dehydrogenases (18). In such
91 yeasts, energy coupling of respiration depends on how regulation of protein synthesis and/or activity
92 determine the distribution of NADH oxidation over Complex I and less efficient systems.

93 The ascomycete budding yeast *Cyberlindnera jadinii* can grow on a variety of carbon sources,
94 including sugars, organic acids and alcohols, and on nitrogen sources including ammonium, nitrate,
95 urea and amino acids (19). Although no extensive quantitative physiology studies have been
96 published on ethanol-grown cultures of *C. jadinii*, this yeast has been reported to show high biomass
97 yields on ethanol ($g_{biomass} \cdot (g_{ethanol})^{-1}$) (16). This observation is consistent with the presence, in the
98 genome of *C. jadinii*, of the genetic information for encoding a Complex I NADH dehydrogenase (20).

99 *C. jadinii* is a polyploid teleomorph of *Candida utilis* (19, 21), which has a long history of safe use in
100 the production of single-cell protein (SCP) for animal nutrition (22) and yeast extracts as a food
101 ingredient (23). Based on dry weight, glucose-grown biomass of *C. jadinii* contains approximately
102 50% protein (16), with an amino acid composition that is compatible with animal nutritional
103 requirements. Nutritional studies have shown that *C. jadinii* SCP can functionally replace
104 conventional protein sources in fish, chicken and swine feed (24-26). *C. jadinii* strains have been
105 reported to grow without vitamin supplementation (27), which enables simple processes and may
106 offer options to select strains with high vitamin contents. SCP has the potential to alleviate negative
107 environmental impacts of food systems (28-31) due to a lower carbon footprint, water use and land
108 usage than those of other protein sources (32).

109 Large-scale industrial production of microbial biomass typically involves aerobic fed-batch cultures.
110 Because of oxygen transfer limitations in industrial bioreactors, achieving high biomass
111 concentrations in such processes requires a decreasing specific growth rate profile (33). For
112 understanding and predicting microbial performance in such industrial contexts, knowledge on
113 growth-rate-dependent physiology, with special attention for maintenance-energy requirements,
114 biomass yields on ethanol and oxygen, and, in the case of SCP production, biomass composition is
115 essential. This study therefore aims to investigate the quantitative physiology of *C. jadinii* with
116 ethanol as a substrate and its implications for SCP production. To this end, we studied growth
117 stoichiometry, growth energetics, vitamin requirements and biomass composition in batch and
118 chemostat cultures of *C. jadinii* strains. Based on quantitative information derived from these
119 experiments, a fed-batch cultivation protocol for SCP production from pure ethanol as carbon
120 source, was designed and conducted at 20-L scale.

121 **Materials & Methods**

122 **Yeast strains and media.** *Cyberlindnera jadinii* strains CBS 621, CBS 567, CBS 841, CBS 842, CBS
123 890, CBS 1516, CBS 1517, CBS 1600, CBS 2160, CBS 4511, CBS 5609, CBS 5947, and CBS 7232 were
124 obtained from the Westerdijk Institute (Utrecht, The Netherlands). *Saccharomyces cerevisiae*
125 CEN.PK113-7D was provided by Dr. Peter Kötter (J.-W. Goethe University, Frankfurt, Germany).
126 Cultures were grown on a synthetic medium (SM) containing 5 $g \cdot L^{-1}$ $(NH_4)_2SO_4$, 3 $g \cdot L^{-1}$ KH_2PO_4 0.5
127 $g \cdot L^{-1}$ $MgSO_4 \cdot 7H_2O$, 15 $mg \cdot L^{-1}$ EDTA, 4.5 $mg \cdot L^{-1}$ $ZnSO_4 \cdot 7H_2O$, 0.3 $mg \cdot L^{-1}$ $CoCl_2 \cdot 6H_2O$, 1 $mg \cdot L^{-1}$
128 $MnCl_2 \cdot H_2O$, 0.3 $mg \cdot L^{-1}$ $CuSO_4 \cdot 5H_2O$, 4.5 $mg \cdot L^{-1}$ $CaCl_2 \cdot 2H_2O$, 3 $mg \cdot L^{-1}$ $FeSO_4 \cdot 7H_2O$, 0.4 $mg \cdot L^{-1}$
129 $Na_2MoO_4 \cdot 2H_2O$, 1 $mg \cdot L^{-1}$ H_3BO_3, 0.1 $mg \cdot L^{-1}$ KI. The pH of the medium was adjusted to 6.0 with 1 M
130 KOH. After autoclaving at 120 °C for 20 min, 1 $mL \cdot L^{-1}$ of a filter-sterilized vitamin solution (0.05 $g \cdot L^{-1}$
131 D-(+)-biotin, 1.0 $g \cdot L^{-1}$ D-calcium pantothenate, 1.0 $g \cdot L^{-1}$ nicotinic acid, 25 $g \cdot L^{-1}$ *myo*-inositol, 1.0 $g \cdot L^{-}$
132 ^{1} thiamine hydrochloride, 1.0 $g \cdot L^{-1}$ pyridoxal hydrochloride, 0.2 $g \cdot L^{-1}$ 4-aminobenzoic acid) (34) was
133 aseptically added. In some experiments, individual or all vitamins were omitted as indicated.
134 Glucose solutions autoclaved at 110 °C for 20 min or pure ethanol were aseptically added to the
135 medium along with the vitamin solution. For strain storage, 30% (v/v) glycerol (final concentration)
136 was added to shake-flask cultures grown overnight at 200 rpm and 30 °C in YPD medium (10 $g \cdot L^{-1}$
137 yeast extract, 20 $g \cdot L^{-1}$ peptone and 20 $g \cdot L^{-1}$ glucose) and 1 mL samples were kept at -80 °C.

138 **Shake flask and microtiter plate cultivation.** Shake-flask cultures, grown in 500-mL flasks
139 containing 100 mL SM supplemented with either 20 $g \cdot L^{-1}$ D-glucose (SMD) or 7.5 $g \cdot L^{-1}$ ethanol (SME),
140 were incubated at 30 °C and 200 rpm in Innova incubators (Brunswick Scientific Edison, NJ). Initial
141 cultures were inoculated from frozen glycerol samples, incubated overnight, and used for a second
142 inoculation in the same medium. Upon reaching early exponential phase, these pre-cultures were
143 used to inoculate a third culture, either in shake flasks or microtiter plates, at an initial OD_{660} of 0.2-
144 1.0. Absorbance at 660 nm (OD_{660}) was measured with a Jenway 7200 spectrophotometer after
145 accurate dilution of samples to yield OD_{660} values between 0.1 and 0.3. Specific growth rates were

146 calculated by fitting exponential phase data (OD 0.2 – 5.0) to the equation $ln\ OD(t) = ln\ OD(0) + \mu_{max} \cdot t$,
147 in which μ_{max} (h^{-1}) represents the maximum specific growth rate. Cultivation in 96-well plates was
148 done in a Growth Profiler 960 (Enzyscreen BV, Heemstede, the Netherlands), operated at 30 °C and
149 at 250 rpm. Image-analysis measurements were taken every 20 min and maximum specific growth
150 rates were calculated from serial dilutions and time courses of green values (35). Mathematical
151 details and assumptions of the method are described in Supp. Material S3.

152 **Chemostat cultivation.** Chemostat cultures of *C. jadinii* and *S. cerevisiae* were grown at 30 °C in 1.5
153 L bioreactors connected to an ez-Control (Applikon Getinge, Delft, The Netherlands). Glucose- and
154 ethanol-limited cultures were grown on SM with 5 $g \cdot L^{-1}$ glucose and 3.75 $g \cdot L^{-1}$ ethanol, respectively,
155 unless otherwise stated, with 0.2 $g \cdot L^{-1}$ Pluronic PE 6100 anti-foaming agent (BASF, Ludwigshafen,
156 Germany). The working volume of cultures was kept at 1.0 L with an electrical level sensor connected
157 to the effluent pump. Unless stated otherwise, culture pH was maintained at 5.0 by automatic
158 addition of 2 M KOH. Cultures were stirred at 800 rpm with 2 Rushton impellers and sparged with air
159 at 0.5 L/min. CO_2 and O_2 contents in the in- and off-gas were measured with a multi-gas analyser
160 (MultiExact 4100 Multi-gas Analyser, Servomex). Dissolved oxygen concentration was monitored
161 with an autoclavable oxygen electrode (Applisens, Schiedam The Netherlands). After inoculation
162 and a batch cultivation phase, the continuous cultivation mode was initiated when a sharp decrease
163 of the CO_2 output indicated substrate depletion. At least two pre-steady-state samples were taken
164 from the effluent line when at least 5 volume changes had passed since the onset of continuous
165 cultivation. When values of dry weight and CO_2 differed by less than 5% for two consecutive volume
166 changes, steady-state samples were collected directly from the culture. Carbon recoveries,
167 calculated based on a yeast biomass carbon content of 45.5% (w/w) (36) were between 95 and 105%
168 unless stated otherwise. Maintenance coefficient and maximum biomass yield on substrate were

169 calculated by linear regression of substrate consumption rates (q_s) plotted against the dilution rate

170 (D) according to the Pirt equation (eq. 1; (37).

171 $$q_s = \frac{D}{Y_{x/s}^{max}} + m_s \quad (1)$$

172 **Fed-batch cultivation.** Fed-batch cultivation was conducted at 30 °C in 20-L Bio Bench reactors

173 (Applikon Getinge, Delft, The Netherlands) with an initial working volume of 8.0 L. Stirrer speed was

174 kept at 800 rpm and pressurised air (20.95% O_2, 0.04% CO_2) was supplied at a flow rate of 7 $L \cdot min^{-1}$.

175 An overpressure of 1.0 bar (2.0 bar total pressure) was applied throughout cultivation to enhance

176 oxygen transfer. A polarographic oxygen electrode (model 32 275 6800; Ingold) was used to monitor

177 the dissolved oxygen concentration to ensure it remained above 15% of air saturation (38).

178 The medium used for fed-batch cultivation contained 2 $g \cdot L^{-1}$ $(NH_4)_2SO_4$, 20 $g \cdot L^{-1}$ KH_2PO_4 6 $g \cdot L^{-1}$

179 $MgSO_4 \cdot 7H_2O$, and trace elements (150 $mg \cdot L^{-1}$ EDTA, 45 $mg \cdot L^{-1}$ $ZnSO_4 \cdot 7H_2O$, 3 $mg \cdot L^{-1}$ $CoCl_2 \cdot 6H_2O$,

180 10 $mg \cdot L^{-1}$ $MnCl_2 \cdot H_2O$, 3 $mg \cdot L^{-1}$ $CuSO_4 \cdot 5H_2O$, 45 $mg \cdot L^{-1}$ $CaCl_2 \cdot 2H_2O$, 30 $mg \cdot L^{-1}$ $FeSO_4 \cdot 7H_2O$, 4

181 $mg \cdot L^{-1}$ $Na_2MoO_4 \cdot 2H_2O$, 10 $mg \cdot L^{-1}$ H_3BO_3, 1 $mg \cdot L^{-1}$ KI) and 0.2 $g \cdot L^{-1}$ Pluronic PE 6100 antifoam.

182 Ammonium hydroxide (25% w/v) was used to control culture pH at 5.0 and to simultaneously provide

183 on-demand nitrogen-source supply. For the initial batch phase, which was inoculated at an OD_{660} of

184 0.2, 12 $g \cdot L^{-1}$ ethanol was used as carbon source. When the end of the exponential growth phase was

185 indicated by a simultaneous decrease of CO_2 production and an increase in the dissolved-oxygen

186 concentration, the fed-batch phase was initiated. During this phase, absolute ethanol was used as

187 carbon source and pumped into the reactor with a controllable Masterflex model 7518-00 pump

188 (Cole-Parmer Instrument Company, Chicago, IL). The feed rate was controlled by a MFCS SCADA

189 Software (Sartorius Stedim Biotech GmbH, Göttingen, Germany) according to equation 2. Over the

190 duration of the fed batch phase, this feed profile resulted in flow rates between 0.006 and 0.050 kg

191 ethanol $\cdot h^{-1}$.

192 $$F_{ethanol}(t) = \left(\frac{\mu}{Y_{x/s}^{max}} + m_s\right) \cdot c_{x,0} \cdot W_0 \cdot e^{\mu \cdot t} \quad (2)$$

193 In equation 2, $F_{ethanol}$ indicates the feed rate of ethanol in kg ethanol $\cdot$ h^{-1}, $c_{x,0}$ the initial biomass
194 concentration ($g_{biomass} \cdot (kg_{broth}^{-1})$), W_0 the initial culture weight (kg_{broth}) and t the time (h) after starting
195 the feed. $Y_{x/s}^{max}$ is the maximum biomass yield on substrate in the absence of maintenance
196 ($g_{biomass} \cdot (g_{ethanol}^{-1})$) and m_s is the maintenance coefficient ($g_{ethanol} \cdot (g_{biomass}^{-1}) \cdot h^{-1}$), both calculated from
197 chemostat experiments. The specific growth rate was kept at 0.10 h^{-1} until the dissolved oxygen
198 concentration decreased to 15% of air saturation. At that point, the feed was changed from
199 exponentially increasing to constant. The fed-batch process was simulated in Python essentially as
200 described by Hensing et al., 1995 (33). The volumetric mass transfer coefficient (k_La) (39) was
201 experimentally determined to be 210 ± 11 h^{-1} with the dynamic technique of absorption (40), and a
202 value of 200 h^{-1} was used for the simulation. Scripts are found in Appendix 1.

203 **Analytical methods.** Biomass dry weight in culture samples was measured as previously described
204 (41). Briefly, dried nitrocellulose filters (pore size 0.45 µm, Gelman Laboratory, Ann Arbor, MI) stored
205 at 80 °C were weighed and used to filter 10.0 mL culture samples. After washing with demineralized
206 water, the filters were dried for 20 min at 350 W output in a microwave (Bosch, Stuttgart, Germany)
207 and weighed again. For determination of metabolite concentrations in culture supernatants,
208 samples were rapidly quenched with cold steel beads and filtered as described by Mashego et al.,
209 2003 (42). Concentrations of glucose and metabolites were determined by HPLC (43). Biomass-
210 specific rates of production and consumption of substrates and products, respectively, as well as
211 carbon recoveries, were calculated with a script available from Appendix 2.

212 **Determination of biomass composition.** Protein content of yeast biomass was determined with
213 the Biuret method according to Verduyn et al., 1991 (14), and lipid content according to Izard &
214 Limberger, 2003 and Johnson et al., 1977 (44, 45) with modifications. Briefly, cell suspension (20 mL)

215 was centrifuged at 10,000 g for 5 min. The pellet was washed and resuspended in demineralized
216 water to give a total volume of 10.0 mL H_2O and stored at -20 °C. For protein measurements, thawed
217 samples were mixed with 3 M NaOH (2:1), boiled at 100 °C for 10 min and cooled on ice. After adding
218 $CuSO_4 \cdot 5H_2O$ (2.5% w/v) to samples (1:3), they were incubated at room temperature for 5 min and
219 centrifuged at 13,000 rpm for 5 min. The absorbance of the clear supernatant was then measured at
220 510 nm. A solution of 5 $g \cdot L^{-1}$ bovine serum albumin (Merck-Sigma A9647) was used to construct a
221 standard curve. For total lipid determination, 100 µL of sample were mixed with 1.0 mL H_2SO_4 and
222 vortexed. Samples were incubated at 100 °C for 10 min and cooled for 5 min. Subsequently, 2.5 mL
223 of phosphoric acid-vanillin reagent (1.2 $g \cdot L^{-1}$ vanillin and 68% phosphoric acid) were added, samples
224 were vortexed and incubated at 37 °C for 15 min. Samples were cooled to room temperature and
225 absorbance was read at 530 nm. Standard solutions of sunflower oil (Merck-Sigma S5007) in
226 chloroform (0 – 1.0 mg/mL) were used to construct a calibration curve. Chloroform was fully
227 evaporated prior to H_2SO_4 addition.

228 To measure RNA and carbohydrate contents of yeast biomass, culture samples were washed once
229 with demineralized water and pellets containing 3 to 5 mg biomass were stored at -20 °C. A 2.0 $g \cdot L^{-1}$
230 solution of yeast RNA (Sigma 10109223001) was prepared in 10 mM Tris-HCl, pH 8.0 and also stored
231 at -20 °C. Before analysis, the stock solution was diluted to obtain standard solutions with RNA
232 concentrations ranging from 5 to 60 $mg \cdot L^{-1}$. RNA was extracted (46) and quantified by measuring
233 absorbance at 260 nm (U-3010 spectrophotometer, Hitachi). Total carbohydrate contents in
234 biomass were quantified according to (47). Briefly, 5 mL of concentrated H_2SO_4 were added to 1 mL
235 of sample, followed by the addition of 1 mL of phenol solution (50 $g \cdot L^{-1}$). Samples were incubated at
236 100 °C for 15 min and subsequently cooled to room temperature. Absorbance was measured at 488
237 nm. As standard solution of glucose and mannose (2:1) was used to construct a calibration range
238 (0.0 - 0.2 $g \cdot L^{-1}$). To correct for the presence of nucleic acid pentoses, relative extinction coefficients

239 of 0.36 and 0.26 versus extinction coefficient obtained from the standard curve were used for RNA
240 and DNA, respectively (adapted from (36)). The following formula was used:

241 $$Abs_{sample} = \varepsilon_{standard} \cdot [carbohydrates] + \varepsilon_{RNA} \cdot [RNA] + \varepsilon_{DNA} \cdot [DNA] \quad (3)$$

242 Where Abs stands for absorbance, $\varepsilon_{standard}$ was obtained from freshly prepared standard curves, RNA
243 content was measured, and DNA content was assumed to be 0.5% of the biomass dry weight for all
244 samples.

245 **Proteome analysis.** Biomass samples (20 mL, containing approximately 3 g biomass·L^{-1}) were
246 centrifuged and washed once with demineralized water. Pellets were resuspended in cold methanol
247 (-20°C) and lysed with a Precellys Homogenizer (Bertin technologies SAS, Montigny-le-Bretonneux,
248 France) at 6,800 rpm for 15 s. Total protein concentrations of the resulting samples were measured
249 by Qubit protein assay, and proteins were isolated by Bligh and Dyer extraction. Isolated proteins
250 were processed further by reduction, alkylation, and trypsin digestion (48). Samples were analysed
251 in technical triplicates by liquid chromatography tandem mass spectrometry (LC-MS/MS) using a
252 Vanquish UHPLC coupled to a Qexactive Plus (Thermo Fisher Scientific, Waltham, USA). Peptides
253 were separated using reverse-phase chromatography with a gradient of water with 0.1% formic acid
254 (solvent A) and 20% water and 0.1% formic acid in acetonitrile (solvent B) from 5% B to 60% B in 52
255 min. Data-independent acquisition (DIA) was performed with a resolution setting of 17,500 within
256 the 400 to 1,200 m/z range and a maximum injection time of 20 ms, followed by high-energy collision-
257 induced dissociation activated (HCD) MS/MS scans with a resolution setting of 17,500 and injection
258 time set to auto. Four DIA MS/MS fragmentation scans were performed after each full scan and the
259 mass range was divided into 100 m/z windows. Raw files were analysed with the Pulsar search
260 engine and Spectronaut, version 17.5, against the annotated proteins of *C. jadinii* (UniProtKB, strain
261 ATCC 18201/CBS 1600 [www.uniprot.org]). Label-free quantification was performed using the top

262 three peptides measured for each protein. Retention time realignment was based on local (non-
263 linear) regression.

264 The obtained signal per protein (*raw signal (i)*, proportional to protein copy number) was multiplied
265 by the respective molecular weight, yielding a *signal (i)*. Subsequently, the *signal (i)* obtained per
266 protein was divided by the sum of all *signals (i)*'s obtained in the sample and multiplied by 100. This
267 resulted in the approximate percentage (in weight/weight) by which each protein contributed to the
268 total proteome mass.

269 **Amino acid analysis.** Culture samples were washed once with demineralized water and pellets
270 containing approximately 50 mg biomass were stored at -20 °C. Total amino acid content of yeast
271 biomass was determined after hydrolysis of the biomass according to the Accq-Tag method
272 (Waters). Before hydrolysis, samples were weighed in a headspace vial, which was subsequently
273 flushed with nitrogen to remove oxygen. Hydrolysis with 6 M HCl was performed to release free
274 amino acids from proteins and peptides. Free amino acids were derivatized on the NH_2 terminus with
275 (AQC) 6-aminoquinolyl-N-hydroxy-succinimidyl carbamate. For complete conversion, samples
276 were incubated for 10 min at 55 °C. Derivatized amino acids were analysed using UPLC reversed-
277 phase chromatography with diode array detection at 260 nm (Acquity UPLC, Waters Corporation,
278 Milford, USA). Derivatized amino acids were chromatographically separated with an Acquity UPLC
279 BEH C18 1.7 µm 2.1*100 mm (Waters) analytical column and a gradient with Mobile phase A:
280 AccQ·Tag Ultra Eluent A, and Mobile phase B: AccQ·Tag Ultra Eluent B, starting at 0.1% B to 9.1% B
281 in 5.74 min increasing to 21.2% B at 7.74 min followed by a ramp to 59.6% B at 8.04 min with a flow
282 rate of 0.7 mL/min. Glutamine, asparagine, tryptophan and cysteine could not be determined with
283 this method because glutamine and asparagine will be converted to glutamic acid and aspartic acid,
284 and tryptophan breaks down during hydrolysis.

285 **Whole-genome sequencing.** Genomic DNA was isolated from culture samples containing
286 approximately $7.0 \cdot 10^9$ cells with the Qiagen 100/G kit (Qiagen, Hilden, Germany), according to
287 manufacturer's instructions. Genomic DNA of *C. jadinii* CBS 621 was sequenced in-house on an
288 Illumina MiSeq sequencer (Illumina, San Diego, CA) to obtain a paired-end library with an insert-size
289 of 550 bp and 300 bp read length using TruSeq Nano DNA library preparation, yielding 6.4 Gb of
290 genomic DNA sequence. *C. jadinii* CBS 5947 was sequenced at Macrogen on an Illumina NovaSeq
291 sequencer to obtain a paired-end library with an insert-size of 550 bp and 151 bp read length using
292 TruSeq DNA PCR-free library preparation, yielding 3.5 Gb of genomic DNA sequence. Reads of
293 strains CBS 621 and CBS 5947 were mapped against the *C. jadinii* NBRC 0988 genome (BioProject:
294 PRJDB11630; GCA_024346625.1) using BWA (version 0.7.15) (49). Alignments were processed using
295 SAMtools (version 1.3.1.) (50) and variants were called by applying Pilon (version 1.18) (51).
296 Heterozygous single-nucleotide polymorphism (SNP) ratios of each chromosome were extracted
297 from the Pilon produced variant calling file (VCF) and the distributions were plotted by using ggplot2
298 (52). *De novo* assembly was performed on the Illumina reads with the SPAdes genome assembler
299 (version 3.9.0) (53). Sequencing data are available at NCBI (https://www.ncbi.nlm.nih.gov/) under
300 the BioProject accession number PRJNA1153750.

301 **Vitamin measurements.** Analyses of selected vitamins (thiamine, pyridoxine, nicotinic acid and
302 riboflavin) were conducted via Elisa by SGS Nederland B.V., division SGS Food Lab. Biomass
303 samples containing circa 3 $g_{biomass}$ were used.

304 **Software and Statistics.** Scripts used for calculations were written in Python (v3.10), using Jupyter
305 Notebook (v 6.4.11). Data visualisation and statistical analysis were conducted in GraphPad Prism
306 (v9.0, GraphPad Software, San Diego, CA).

307

308 **Results**

309 **1. Biomass yield and protein content in glucose- and ethanol-grown chemostat cultures**

310 To verify earlier reports that *C. jadinii* shows higher biomass yields on ethanol than *S. cerevisiae* (14,
311 16), aerobic ethanol-limited chemostat cultures of *C. jadinii* CBS 621 and *S. cerevisiae*
312 CEN.PK113-7D were grown at a dilution rate of 0.10 h^{-1}. Consistent with earlier reports (16),
313 steady-state cultures of *S. cerevisiae* CEN.PK113-7D showed a biomass yield of 0.59 ± 0.01
314 $g_{biomass} \cdot (g_{ethanol})^{-1}$ (Fig 1A). In four independent chemostat cultures of *C. jadinii* CBS 621, biomass yields
315 were consistently 23% higher (0.74 ± 0.01 $g_{biomass} \cdot (g_{ethanol})^{-1}$) than in those of *S. cerevisiae*. The
316 biomass yields on ethanol of *C. jadinii* CBS 621 were higher than previously reported for chemostat
317 cultures of this strain (0.69 $g_{biomass} \cdot (g_{ethanol})^{-1}$) (14, 16). In contrast to the ethanol-limited cultures,
318 glucose-limited chemostat cultures of *C. jadinii* CBS 621 and *S. cerevisiae* CEN.PK113-7D showed
319 only 6% difference in biomass yield (0.51 ± 0.01 $g_{biomass} \cdot (g_{glucose})^{-1}$ and 0.48 ± 0.00 $g_{biomass} \cdot (g_{glucose})^{-1}$,
320 respectively; Fig 1A). Both species showed lower biomass yields on oxygen in ethanol-limited
321 cultures than in glucose-limited cultures (Fig 1B). However, biomass yields on oxygen in ethanol-
322 limited cultures of *C. jadinii* were approximately 50% higher in *C. jadinii* than *S. cerevisiae* (Table S1).
323 The different biomass yields of *C. jadinii* and *S. cerevisiae* on ethanol may reflect the presence and
324 absence, respectively, of a proton-pumping respiratory complex I in these two yeast species (14, 20).

325 Consistent with earlier reports (16, 36), the highest protein content in yeast biomass (0.54
326 $g_{protein} \cdot (g_{biomass})^{-1}$) was observed in the ethanol-limited *C. jadinii* cultures and the lowest protein
327 content in the glucose-limited *S. cerevisiae* cultures (0.36 $g_{protein} \cdot (g_{biomass})^{-1}$) (Fig 1C). In the ethanol-
328 limited cultures of *C. jadinii*, the protein yield on ethanol reached 0.40 $g_{protein} \cdot (g_{ethanol})^{-1}$ (Fig 1D).

329 **2. Proteome and amino-acid composition of ethanol-grown *C. jadinii***

330 To further investigate the biomass composition of the ethanol- and glucose-limited chemostat
331 cultures of *C. jadinii*, proteome analyses were performed. Of 2596 detected proteins, 1656 were
332 identified with at least 3 different peptides (Supp. Material S1). In the ethanol-limited *C. jadinii*
333 cultures, the 10 most abundant proteins comprised approximately 25% of the proteome. Two
334 isoforms each of alcohol dehydrogenase (*Cj*Adh) and acetaldehyde dehydrogenase (*Cj*Ald), as well
335 as an acetyl-CoA synthetase 1 (*Cj*Acs1), which together catalyse the first three steps in ethanol
336 catabolism (Fig 1E), accounted for 6 of the 10 most highly abundant proteins (Fig 1F). Key proteins in
337 ethanol assimilation (isocitrate lyase and malate synthase) were also very highly expressed. While
338 their levels were clearly higher in ethanol-grown cultures, the 6 proteins involved in ethanol
339 catabolism were also abundant in glucose-grown cells (Fig 1F). In contrast, levels of elongation
340 factor 1-α and the α-subunit of the F_1F_o-ATP synthase were similar in glucose-limited and ethanol-
341 limited cultures (Fig 1F).

342 In view of the 75% higher respiration rate in ethanol-limited cultures than in glucose-limited cultures
343 of *C. jadinii* CBS 621 (4.4 vs 2.5 mmol $O_2 \cdot (g_{biomass})^{-1} \cdot h^{-1}$, Table S1), levels of proteins involved in
344 oxidative phosphorylation were also investigated. A set of 71 proteins involved in oxidative
345 phosphorylation that were represented by at least 2 independent peptides and included subunits of
346 all 4 respiratory complexes and ATP synthase (Supp. Material S1) showed, on average, a 60% higher
347 level in ethanol-limited cultures than in glucose-limited cultures. Complex I subunits (28 detected)
348 were, on average, 75% higher in ethanol- compared to glucose-limited samples (Fig. S1A).

349 The amino acid composition of *C. jadinii*, which is important for food and feed applications of
350 microbial biomass (54), was analysed and compared to that of *S. cerevisiae*. Biomass from ethanol-
351 and glucose-grown chemostat cultures of the two yeasts showed similar amino acid composition,
352 with high glutamate and glutamine levels (Table S2). A low content of methionine in glucose- and
353 ethanol-grown chemostat cultures of both yeasts (1.35 to 1.80% of the proteome, Fig 1G) was

354 previously reported for multiple yeasts species (24). The sum of the analysed amino acid contents
355 followed the same trend as total protein measurements (Fig S1B) but resulted in lower absolute
356 values (Fig S1C). There is a growing interest in using yeast biomass in aquaculture to produce fish
357 feed and thereby to curtail overfishing for fishmeal (24, 28, 54). A comparison of amino acid levels in
358 ethanol-grown *C. jadinii* biomass with reference values for essential amino acids in fish feed
359 identified methionine as limiting (Fig S1D), with all other amino acids at or above required levels.

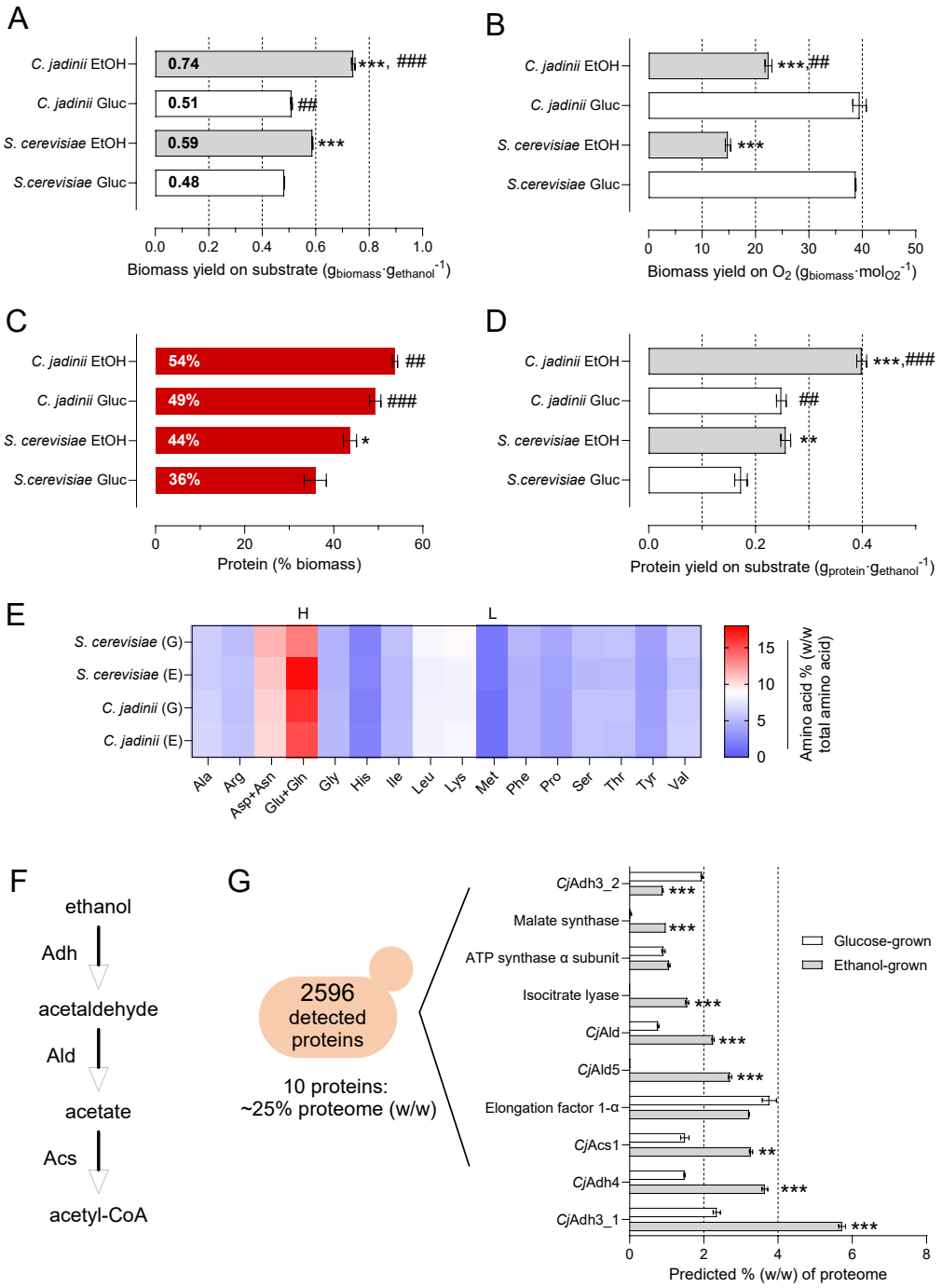

360

361 **Figure 1: Effect of growth-limiting carbon source on the physiology of *C. jadinii* and proteome**
362 **composition.** *S. cerevisiae* CEN.PK113-7D and *C. jadinii* CBS 621 were grown in steady-state, aerobic
363 ethanol-limited and glucose-limited chemostats at a dilution rate of 0.10 h^{-1}. **(**A, B) Biomass yields on substrate
364 and oxygen, respectively. (C) Protein content as a percentage of biomass. (D) Protein yields on substrate. (E)

365 Enzymes involved in conversion of ethanol to acetyl-CoA. Adh: alcohol dehydrogenase, Ald: aldehyde
366 dehydrogenase, Acs: acetyl-CoA synthetase. (F) Top 10 most abundant proteins (with at least 3 identified
367 peptides) in the proteome of ethanol-grown *C. jadinii* versus the levels of the same proteins in glucose-limited
368 chemostats in the same species. *Cj* stands for *Cyberlindnera jadinii*. (G) Protein amino acid residue
369 composition (as a percentage of the total amino acid residue pool. H stands for highest, and L for lowest amino
370 acids in abundance for all analysed species and conditions. #p<0.05, ##p<0.01, ###p<0.001, *S. cerevisiae* vs
371 *C. jadinii*, same substrate. *p<0.05, **p<0.01, ***p<0.001, same yeast species, ethanol- (EtOH) vs glucose-
372 grown (Gluc), n=2.

373

374 **3. Maximum biomass yield and maintenance-energy requirement of *C. jadinii* in ethanol-limited**
375 **chemostat cultures**

376 To analyse how specific growth rate affects biomass yield and to estimate the maintenance energy
377 requirements of *C. jadinii* CBS 621, ethanol-limited chemostat cultures were grown at different
378 dilution rates. To define a range of dilution rates, maximum specific growth rates (μ_{max}) of *C. jadinii*
379 were determined in batch cultures grown on synthetic medium with ethanol or glucose as sole
380 carbon source (Fig 2A). Values of μ_{max} on ethanol and glucose were 0.43 ± 0.01 h^{-1} and 0.57 ± 0.01 h^{-1},
381 respectively (Fig 2B). Both values are higher than the reported μ_{max} of *S. cerevisiae* CEN.PK113-7D on
382 synthetic medium with glucose (0.39 h^{-1}) (55).

383 Ethanol-limited chemostat cultures of *C. jadinii* were grown at dilution rates ranging from 0.025 to
384 0.30 h^{-1}. Over this range of specific growth rates, biomass yields on ethanol ranged from 0.59 to 0.81
385 $g_{biomass} \cdot (g_{ethanol})^{-1}$ (Fig 2C, Table S3). Using the Pirt equation (eq. 1), we derived maximum biomass
386 yields on ethanol and oxygen based on the linear fits shown in Fig 2D-E. From the same data,
387 maximum biomass yields of 0.83 $g_{biomass} \cdot (g_{ethanol})^{-1}$ and 28 $g_{biomass} \cdot (mol\ O_2)^{-1}$ on oxygen were

388 determined. The maximum yield on ethanol is very close to a theoretical value of 0.84
389 $g_{biomass} \cdot (g_{ethanol})^{-1}$, estimated based on the assimilation equation for ethanol by *C. jadinii* (14). This
390 observation suggests that, at high specific growth rates, growth of *C. jadinii* CBS 621 is close to being
391 carbon-limited rather than energy-limited. From Fig 2D-E, we derived maintenance coefficients for
392 ethanol (m_s) and oxygen (m_{O2}) of 0.28 $mmol_{ethanol} \cdot (g_{biomass})^{-1} \cdot h^{-1}$ and 0.76 mmol $O_2 \cdot (g_{biomass})^{-1} \cdot h^{-1}$,
393 respectively (Fig 2F). Maintenance coefficients relate to use of energy substrate for processes that
394 are not associated with growth, such as homeostasis of membrane potential and turnover of cellular
395 components (56) and explains the decline in biomass yield as the dilution rate approaches zero (Fig
396 2C). Assuming an *in vivo* P/O ratio of 1.8 *for C. jadinii* (14) and growth-rate independent maintenance-
397 energy requirements ((37), Eq. 1), we estimated an ATP requirement for maintenance (m_{ATP}) of 2.7
398 mmol ATP $\cdot$ (g biomass)$^{-1} \cdot h^{-1}$ (Fig 2F). This value is over 4-fold higher than the estimated m_{ATP} for *S.*
399 *cerevisiae* grown aerobically in glucose-limited cultures (0.63 $mmol_{ATP} \cdot (g_{biomass}^{-1}) \cdot h^{-1}$) (57).

400 A previous publication reported that *C. jadinii* shows higher biomass yields at pH 4.0 than at pH 5.0
401 (58). However, we did not observe a meaningful change in biomass yield when ethanol-limited
402 cultures were grown at pH 4.0 instead of 5.0, while protein contents of cultures grown at pH 4.0 were
403 lower (Fig S2A-C). Co-feeding with formic acid, whose metabolism in yeasts is strictly dissimilatory,
404 can supply additional NADH and thereby increase ATP availability for assimilation of the carbon
405 source (16, 59, 60). Formic acid co-feeding only marginally increased the biomass yield and protein
406 content in ethanol-limited cultures, resulting in a protein yield on ethanol of 0.43 $g_{protein} \cdot (g_{ethanol})^{-1}$ (Fig
407 S2D-F). The effect of formic acid co-feeding was more pronounced in glucose-grown chemostat
408 cultures, in which protein yields on glucose increased from 0.25 to 0.33 $g_{protein} \cdot (g_{glucose})^{-1}$ (Fig S2F-H).

409 **4. Impact of specific growth rate on protein content and alcohol dehydrogenase levels in**
410 **ethanol-limited chemostat cultures**

411 In aerobic, glucose-limited chemostat cultures of yeasts, the protein content of the biomass
412 typically increases with increasing specific growth rate (36, 58, 61, 62). In contrast, aerobic ethanol-
413 limited chemostat cultures of *C. jadinii* CBS 621 showed slightly higher protein contents at specific
414 growth rates below 0.10 h^{-1} (Fig 2G). Similarly, while RNA content was reported to positively correlate
415 with specific growth rate in *S. cerevisiae* (36, 63), ethanol-limited chemostat cultures of *C. jadinii*
416 CBS 621 showed essentially stable RNA contents across a range of dilution rates (Fig 2G). In contrast
417 to protein and RNA contents, contents of carbohydrates and lipids in biomass increased with
418 specific growth rate, representing 26 and 11%, respectively, of the biomass at D = 0.30 h^{-1} (Fig. 2H).
419 Yields of all four macromolecular biomass components on ethanol showed a growth-rate dependent
420 increase (Fig S2G-H), reflecting the trend of total biomass yields (Fig 2C).

421 Many studies report that the fraction of microbial proteomes allocated to the translation machinery
422 increases with increasing specific growth rate (64-66). To investigate whether ethanol-grown *C.*
423 *jadinii* exhibited a similar correlation, proteomics analyses were performed on samples from
424 cultures grown at 0.025, 0.10, 0.21 and 0.30 h^{-1}. The resulting proteome dataset (Supp. Material S2)
425 was manually curated into 7 categories based on the Gene Ontology annotation obtained from
426 UniProt (67). Levels of 357 proteins correlated well with specific growth rate ($R^2 > 0.90$; 273 positive
427 and 84 negative correlations; Supp. Material S2). The most prominent effect was a negative
428 correlation of the abundance of proteins involved in ethanol catabolism (*Cj*Adh, *Cj*Ald and *Cj*Acs)
429 with growth rate. These proteins occupied approximately 27% of the proteome at 0.025 h^{-1} and 12%
430 at 0.3 h^{-1}. In contrast, the fraction of proteins involved in oxidative phosphorylation (OXPHOS)
431 increased from 4.8 to 7.4% (Fig. 2I), which positively correlated with oxygen consumption rates (Fig
432 S3A). These abundances are similar to a predicted proteome contribution of OXPHOS proteins of
433 approximately 5% in *S. cerevisiae* and *Issatchenkia orientalis* (*Pichia kudriavzevii*) (64, 68). The
434 fractions of TCA-cycle enzymes and proteins involved in amino acid synthesis both increased from

435 approximately 4% at 0.025 h^{-1} to 9% at 0.3 h^{-1}, while the fraction of the proteome allocated to the
436 translation machinery increased from 22 to 29% (Fig 2I).

437 Of the proteins involved in ethanol catabolism, *Cj*Adh had the strongest impact on the composition
438 of the proteome. Total *Cj*Adh levels (3 most abundant isoforms, Fig S3B) accounted for 17% and 5%
439 of the proteome at 0.025 h^{-1} and 0.3 h^{-1}, respectively (Fig 2J), followed by *Cj*Ald and *Cj*Acs (Fig S3C-
440 D). Given the almost linear correlation between *Cj*Adh levels and dilution rate, we estimated *Cj*Adh's
441 specific maximum activity (v_{max}). When these estimates were plotted against measured biomass-
442 specific ethanol consumption rates (which should equal the *in vivo* flux through *Cj*Adh), the curves
443 intercepted at D = 0.39 h^{-1} (Fig 2K), which is very close to the maximum specific growth rate of *C.*
444 *jadinii* on ethanol (0.43 h^{-1}). This comparison suggests that the maximum specific growth rate of *C.*
445 *jadinii* CBS 621 on ethanol may be constrained at the proteome by the level of alcohol
446 dehydrogenase.

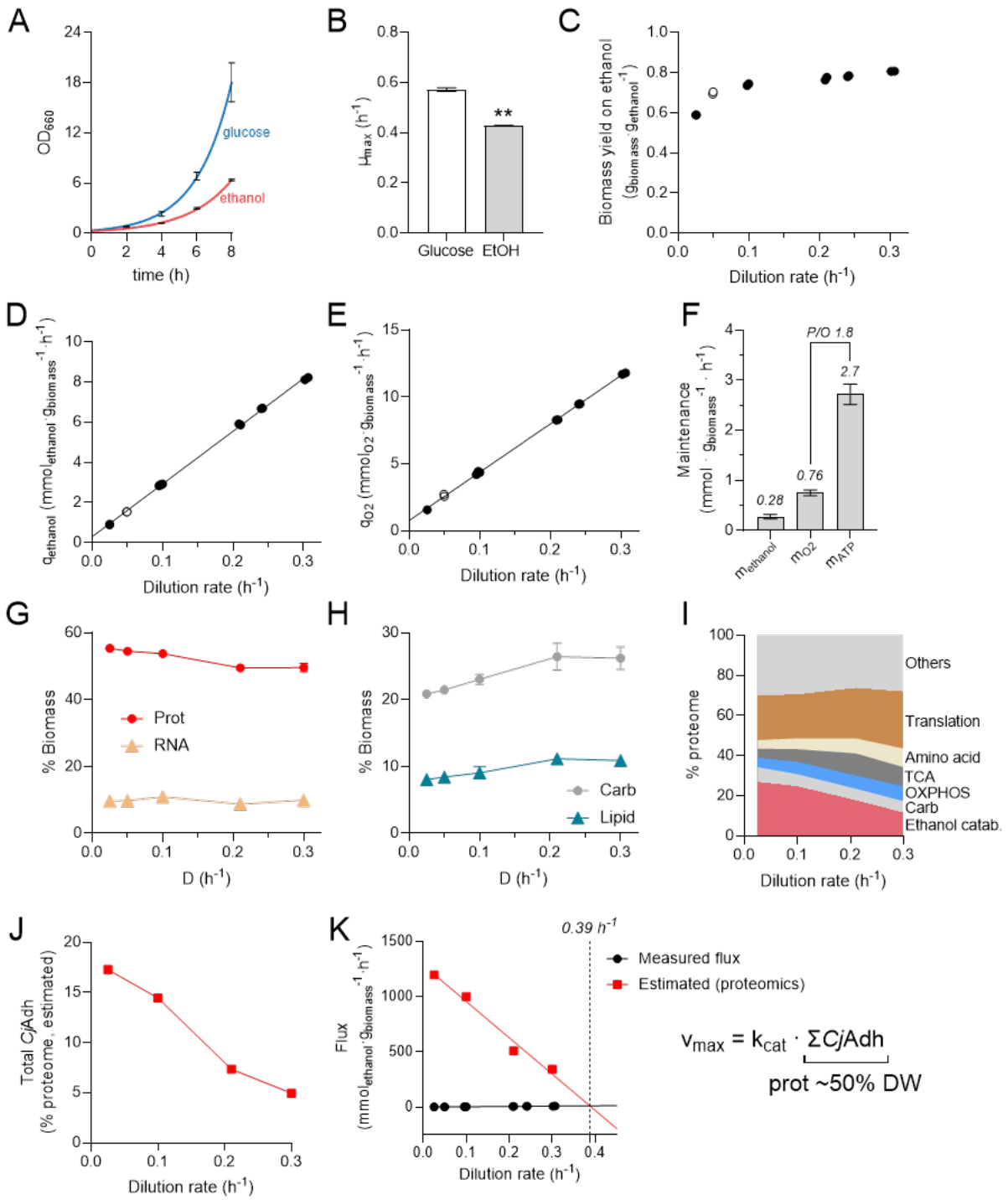

447

448 **Figure 2: Physiology of *C. jadinii*, biomass composition, and proteome in ethanol-limited cultures at**

449 **different dilution rates.** (A) Optical density at 660 nm (OD_{660}) as a function of time and (B) maximum growth

450 rates (μ_{max}) of glucose- and ethanol-grown batch cultures. (C) Biomass yield on ethanol, (D) biomass-specific

451 ethanol uptake rate ($q_{ethanol}$) and (E) biomass-specific oxygen uptake rates (q_{O_2}) in aerobic, steady-state,
452 ethanol-limited chemostat cultures of *C. jadinii* CBS 621. (F) Maintenance requirements for ethanol ($m_{ethanol}$)
453 and oxygen (m_{O2}) calculated as the y-intercept of the fitted curves shown in D and E, respectively. Maintenance
454 ATP requirements (m_{ATP}) were estimated from $m_{O2,}$ assuming an *in vivo* P/O ratio of 1.8 (14). (G) and (H)
455 Quantification of the main components of the biomass in % of dry weight: proteins (Prot), RNA, carbohydrates
456 (Carb) and lipids. (I) Protein allocation in ethanol-limited chemostat cultures grown at different dilution rates.
457 Categories were manually curated and represent (in ascending order) Ethanol catabolism (first three steps
458 shown in Fig 1F), Carbohydrate metabolism (Carb.), Oxidative Phosphorylation (OXPHOS), TCA cycle
459 (including the glyoxylate shunt reactions), Amino acid metabolism, Translation and Others. The last category
460 encompasses proteins from pathways with a lower proteome allocation or for which no pathway was assigned.
461 (J) Total alcohol dehydrogenase protein (*Cj*Adh, % of proteome) as a function of dilution rate. (K) Estimated v_{max}
462 for *Cj*Adh, assuming a k_{cat} of 150 min^{-1} for all isoforms (Brenda database (69), EC 1.1.1.1, average reported
463 value for yeasts) and a proteome comprising 50% of the dry weight (w/w), plotted together with the ethanol
464 consumption rates ($q_{ethanol}$) from bioreactor experiments. 0.39 h^{-1} represents the intersection between both
465 lines. Open symbols show carbon recovery of around 107%, while closed symbols represent carbon
466 recoveries of 100±5%. **$p<0.001$, n=2.

467

468 **5. *C. jadinii* CBS 621 is a thiamine auxotroph**

469 The chemically defined medium used in the experiments described above contained seven B-type
470 vitamins that are commonly included in defined media for yeast cultivation (70). However, although
471 vitamin-independent growth of other *C. jadinii* strains has been reported (27), the vitamin
472 dependence of strain CBS 621 has not been investigated. To assess vitamin requirements of this
473 strain, it was grown in shake-flask cultures on 'dropout' synthetic media from which a single vitamin
474 was omitted. In addition, growth was measured on a synthetic medium from which all 7 vitamins
475 were omitted (Δvitamins). In these experiments, only the Δthiamine and Δvitamins media showed

476 severely compromised growth (Fig 3A-B). When, after 24 h incubation in vitamin-free medium with
477 ethanol, culture samples were used to inoculate new flasks, the growth deficiency after 24 h further
478 incubation in vitamin-free medium was even more pronounced (Fig 3B). Addition of thiamine
479 sufficed to restore growth (Fig 3C).

480 To investigate the apparent thiamine auxotrophy *C. jadinii* CBS 621, its genome was sequenced and
481 *de novo* assembled. The estimated genome size of 17.9 Mb (Table S4) is larger than that of other *C.*
482 *jadinii* strains (19). This may be due to its high degree of heterozygosity, which generated alternative
483 alleles for heterozygous regions during assembly. Based on the distribution of SNPs in the
484 heterozygous regions across the genome, CBS 621 is most probably triploid (Fig S4A). A search for
485 genes encoding proteins in thiamine biosynthesis (*CjTHI4*, *CjTHI5*, *CjTHI6* and *CjTHI20*) (70) was
486 performed in UniProt, using *C. jadinii* as a taxonomy identifier. The annotated amino acid sequences
487 for the type strain CBS 1600 were then used to identify homologs in strain CBS 621 with the BLAST
488 tool (Fig 3D). This homology search yielded matches in strain CBS 621 with *CjTHI5*, *CjTHI6* and
489 *CjTHI20*, but not with *CjTHI4*, which encodes thiamine thiazole synthase, a single-turnover 'suicide
490 enzyme' (70) involved in thiamine biosynthesis. Based on these results, we concluded that loss of
491 the *CjTHI4* gene rendered *C. jadinii* CBS 621 a thiamine auxotroph.

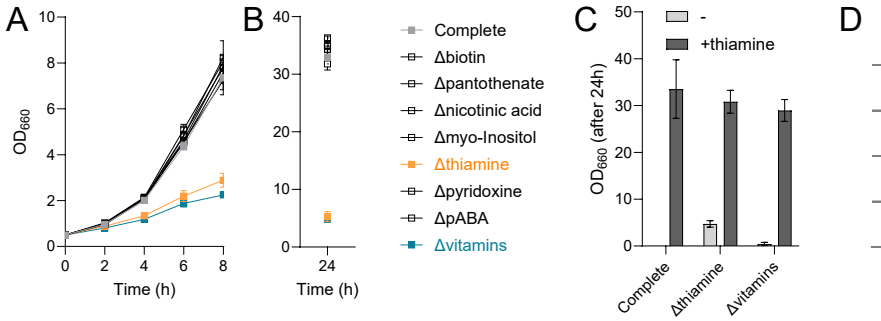

Gene query Strain: CBS 1600	Match identify (E value) Strain: CBS 621
THI4 GenBank: CEP22926-1	No hit
THI5 GenBank: CEP24253-1	99.61% (0)
THI6 GenBank: CEP24456-1	97.01% (0)
THI20 GenBank: ODV74287-1	98.96% (0)

492

493 **Figure 3: Growth of *C. jadinii* CBS 621 on single-vitamin dropout and vitamin-free media.** (A) Growth curves
494 of *C. jadinii* CBS 621 on single-vitamin dropout media in shake flasks grown on synthetic medium with ethanol

495 as a sole carbon source. Δ"vitamin name" indicates absence of only the indicated vitamin from the standard
496 vitamin mix. *Complete* indicates presence of all vitamins and *Δvitamins* indicates absence of all vitamins. (B)
497 OD_{660} after 24h of cultivation in shake flasks. (C) OD_{660} after further 24h of cultivation in shake flasks for
498 samples from indicated groups (x-axis) that were reinoculated at OD 0.5 in the presence or absence of
499 thiamine, n=2. (D) Overview of tBLASTn search to identify genes coding for enzymes in the biosynthesis of
500 thiamine in CBS 621. The reference GenBank IDs used as queries were retrieved from UniProt, based on
501 searches containing the respective protein name and species (*C. jadinii* CBS 1600). The tBLASTn algorithm was
502 run locally using default settings.

503

504 **6. Cultivation of prototrophic *C. jadinii* strains on ethanol on a vitamin-free medium**

505 To explore growth of prototrophic *C. jadinii* strains on ethanol, twelve additional strains were
506 selected based on availability of genome sequences and isolation origin. These strains were then
507 evaluated for (i) vitamin dependency, (ii) specific growth rate, and (iii) biomass and protein yields in
508 ethanol-grown cultures. A serial-dilution based method (Fig 4A) was used to calculate specific
509 growth rates in microtiter plates (35). When plotting the natural logarithm of the dilution factor
510 against the time to reach a predefined threshold cell concentration, the specific growth rate
511 corresponds to the slope of the curve (Fig 4B). Of the tested *C. jadinii* strains, only CBS 621 and CBS
512 7232 fail to grow on vitamin-free medium (Fig 4C). Growth of these strains was rescued by adding of
513 thiamine and biotin, respectively (Fig S5A). The maximum specific growth rates of the strains ranged
514 from 0.13 - 0.44 h^{-1} (Fig 4C). Most of the variation in the dataset could be attributed to strain
515 differences ($p<0.001$). Vitamin absence also significantly impacted the specific growth rates, leading
516 to an average 10-15% lower growth rate ($p<0.001$) (Fig 4C). The final Green Value of the growth curves
517 (Fig S5B) showed less variation among samples.

518 Three *C. jadinii* strains were selected for further investigation: CBS 5609 (highest μ_{max}), CBS 1600
519 (largest difference in μ_{max} caused by vitamin absence) and CBS 5947 (among the top three strains
520 with the highest final Green Value). Maximum specific growth rates of these three strains were
521 measured in shake flasks to validate the serial dilution method. Although the effect of vitamin
522 absence on CBS 1600 was less pronounced (Fig 4D), values obtained with the two methods
523 corresponded well (Fig 4E, S5C). Publicly available genome sequences from strains CBS 1600 and
524 CBS 5609 (21, 71), indicated the presence of a complete *THI4* gene. Presence of *THI4* in strain CBS
525 5947 was confirmed by whole-genome sequencing (Table S4). Like strains CBS 5609 and CBS 621,
526 *C. jadinii* CBS 5947 appeared to be triploid based on its SNP distribution (Fig S4B).

527 To investigate biomass yields and protein contents of the three selected strains during growth on
528 ethanol in vitamin-free medium, they were grown in ethanol-limited chemostats at 0.10 h^{-1} in the
529 absence of supplemented vitamins (Table S5). *C. jadinii* CBS 5609, the strain with the highest μ_{max} on
530 ethanol (0.46 h^{-1}, Fig 4D) showed the lowest biomass yield on ethanol and oxygen (Fig 4F-G). Strains
531 CBS 1600 and CBS 5947 showed nearly the same biomass yields on ethanol (0.72 and 0.74
532 $g_{biomass} \cdot (g_{ethanol})^{-1}$, respectively (Fig 4F-H). All three strains showed a protein content of approximately
533 54% (Fig 4H). Vitamin-supplemented ethanol-limited cultures of strains CBS 1600 and CBS 621
534 showed the same biomass yield on ethanol and protein content (Fig 4F-H). For strain CBS 1600,
535 these results indicate that omitting vitamins from synthetic media does not affect biomass yield and
536 protein content during ethanol-limited growth at 0.10 h^{-1}.

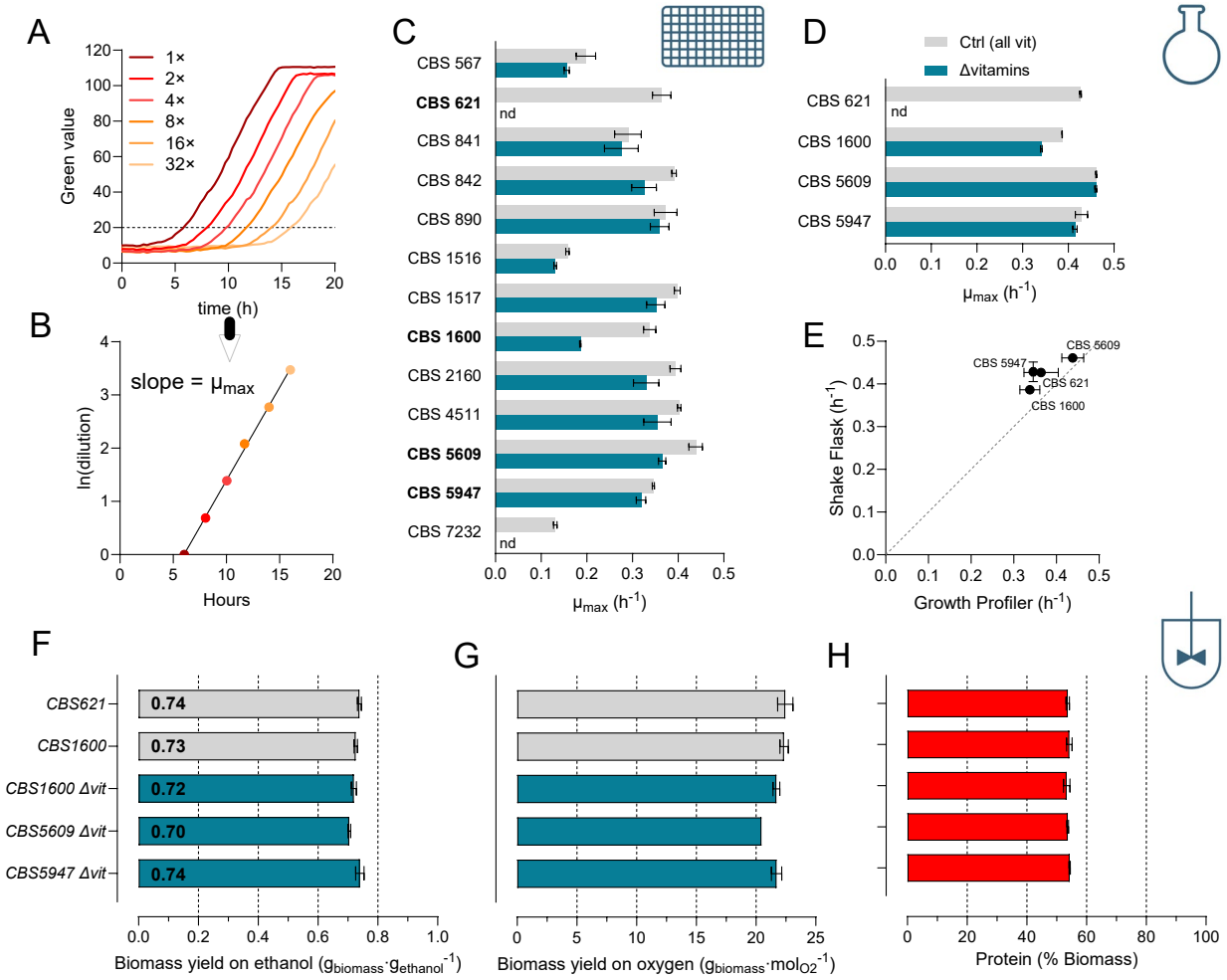

Figure 4: Characterization of *C. jadinii* strains in microtiter plates, shake flasks and bioreactors concerning vitamin dependency. (A) Representative growth curves of serially diluted CBS 621 in microtiter plates, ranging from 1 to 32× dilution, initial OD_{660} 0.2 to 0.00625, respectively. (B) Calculation of specific growth rates via serial dilution method. The time (h) required for a specific dilution to reach a green value of 20 was plotted against the natural logarithm of the respective dilution (1-32). (C) Specific growth rates for 13 *C. jadinii* strains grown on ethanol in the presence or absence of vitamins, calculated with the serial dilution method, n.d: non-detectable. (D) Specific growth rates of 4 *C. jadinii* strains grown on ethanol in shake flasks in the presence or absence of vitamins. (E) Correlation of specific growth rates obtained in microtiter plates (x-axis) with those measured in shake flasks (y-axis) for strains grown in the presence of vitamins. (F-H) Biomass

547 yields on ethanol, oxygen and protein content for selected strains grown in ethanol-limited chemostats
548 (dilution rate 0.10 h^{-1}). Where indicated by Δvit, no vitamins were added to the cultivation, n=2-3.

549

550 **7. High-cell-density fed-batch cultivation of *C. jadinii* on ethanol in a mineral, vitamin-free**
551 **medium.**

552 Of the vitamin-prototrophic *C. jadinii* strains, CBS 5947 showed the highest biomass yield in ethanol-
553 limited chemostat cultures (0.74 $g_{biomass} \cdot (g_{ethanol})^{-1}$, Fig 4F). To evaluate whether this strain could be
554 grown to high biomass densities on ethanol in a vitamin-free medium, a fed-batch protocol was
555 developed. After an initial batch phase on 12 $g \cdot L^{-1}$ ethanol, a biomass concentration of 5.5
556 $g_{biomass} \cdot (kg_{broth})^{-1}$ was reached in two independent reactors. For the subsequent fed-batch regime,
557 pure ethanol was continuously fed and 25% NH_4OH was used as pH titrant and nitrogen source. To
558 increase oxygen solubility, 1 bar overpressure was applied (Fig 5A). The initial specific growth rate
559 was set at 0.10 h^{-1} by applying a preprogrammed exponentially increasing ethanol feed rate (Fig 5B).
560 When dissolved oxygen concentration in the reactor decreased to a concentration corresponding to
561 15% of air saturation at atmospheric pressure (Fig S6A), the ethanol feed rate was first fixed at 0.047
562 $kg_{ethanol} \cdot h^{-1}$ and, after 5 additional hours, at 0.035 $kg_{ethanol} \cdot h^{-1}$ (Fig 5B) to prevent oxygen limitation. In
563 total, approximately 1.4 kg of ethanol was consumed in each reactor within 48 h (Fig 5C), leading to
564 biomass concentration of 98 ± 4 $g_{biomass} \cdot (kg_{broth})^{-1}$ (Fig 5D). Consistent with the cultures being ethanol-
565 limited, the ethanol concentration in culture samples remained below detection limit throughout the
566 fed-batch phase. From the time-dependent increase of the amount of biomass in the reactor, we
567 calculated an approximate specific growth rate of 0.02 h^{-1} at the end of the fed-batch phase (Fig 5E).
568 A decline in growth rate was also evident from the slope of the CO_2 profile during fermentation (Fig
569 S6B). The fed-batch process was simulated (33) based on the parameters calculated from Fig 2D-F

570 and the feed profile shown in Fig 5B. Experimentally determined specific growth rates and ethanol
571 consumption were consistent with model predictions (Fig 5C-E).

572 The protein content remained at 50% during the exponential feed phase of the fed-batch culture (Fig
573 5F). However, in contrast to observations in steady-state chemostat cultures (Fig 2) in which protein
574 concentrations did not decline at low specific growth rates, a decrease of the protein content to 42%
575 was observed towards the end of the fed-batch cultures (Fig 5F). This indicates that the protein
576 content decreases when the growth rate was dynamically changed from 0.10 to 0.022 h^{-1}. In the two
577 fed-batch experiments, an average of 405 g protein was produced (Fig 5G). Based on the total
578 ethanol consumed and total biomass and protein produced during the fed-batch phase, biomass,
579 and protein yields of 0.65 $g_{biomass} \cdot (g_{ethanol})^{-1}$ and 0.28 $g_{protein} \cdot (g_{ethanol})^{-1}$, respectively, were calculated (Fig
580 5H). Production of low concentrations of acetate and succinate in the fed-batch processes (~10 mM
581 final concentrations) (Fig S6C) played a negligible role in the total carbon recovery (Fig S6D-E).

582 In the fed-batch cultures, strain CBS 5947 needed to synthesize vitamins to sustain growth. Levels
583 of thiamine, riboflavin, niacin, and pyridoxine in fed-batch grown *C. jadinii* CBS 5947 ranged from 1.7
584 – 260 mg $\cdot (kg_{biomass})^{-1}$. When compared with the vitamin contents in aquaculture diets (Table S6) (72),
585 ethanol-grown *C. jadinii* biomass showed higher levels of niacin, riboflavin and pyridoxine, while
586 thiamine content of the yeast biomass was approximately 3-fold lower.

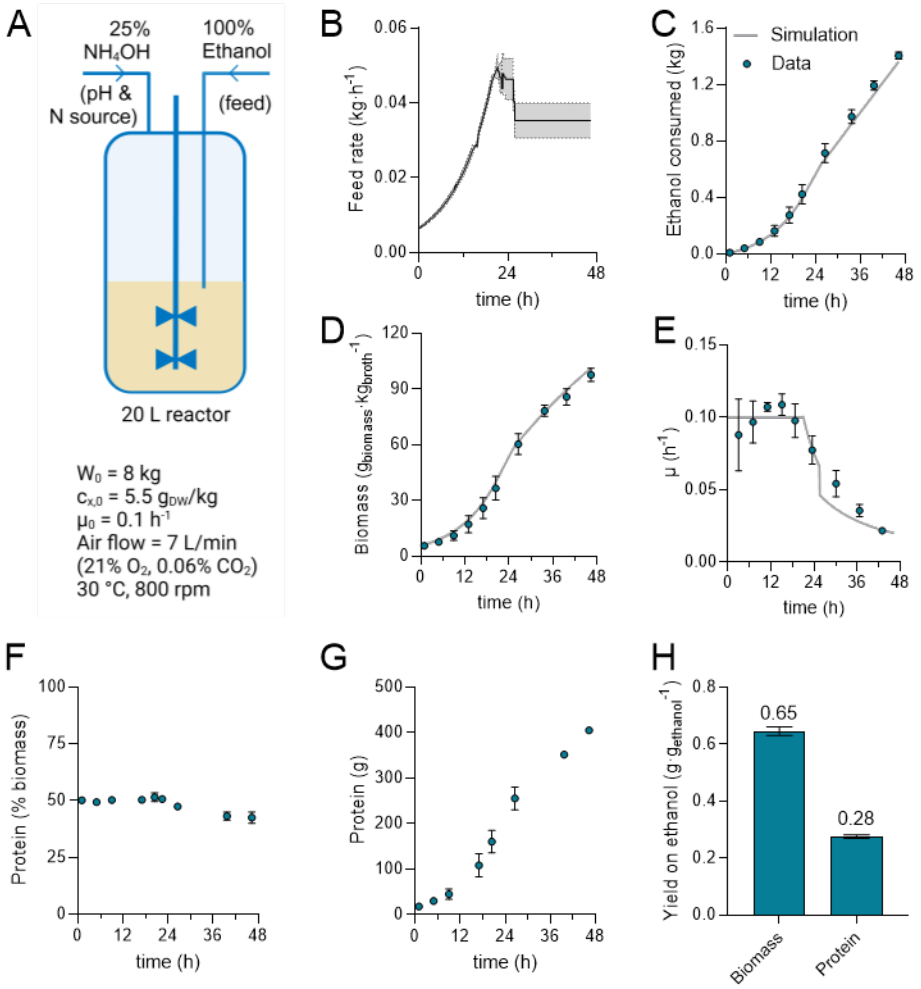

587

588 **Figure 5: Growth of *C. jadinii* CBS 5947 on vitamin-free medium in aerobic, ethanol-limited fed-batch**
589 **cultures.** Aerobic fed-batch fermentation was performed at 30 °C, at pH 5.0 and at 1 bar overpressure, with a
590 feed of pure ethanol. A 25% (w/v) solution of NH_4OH solution was used for simultaneous pH control and
591 nitrogen supplementation. (A) Scheme of reactor and critical parameters related to the process (fed-batch
592 phase). W_0: initial weight of the culture broth (kg), $c_{x,0}$: initial biomass concentration ($kg_{biomass} \cdot (kg_{broth})^{-1}$), μ_0:
593 initial specific growth rate in fed-batch phase (h^{-1}), DW = biomass dry weight concentration (g biomass · (kg
594 broth)$^{-1}$), created with BioRender.com. (B) Profile of feed rate during the fed-batch phase. (C-E) Consumed
595 ethanol, biomass dry weight, and growth rate (μ) during the fed-batch phase. Symbols represent data and grey
596 lines refer to simulations. (F-G) protein percentage in the biomass and total protein content during the fed-

597 batch phase. (H) Total biomass and protein yield on ethanol based on the whole fed-batch process. Data are
598 shown for 2 independent reactors (mean ± SD).

599

600 **Discussion**

601 Fast growth of industrial micro-organisms is especially beneficial during batch cultivation and during
602 the initial exponential growth phase of aerobic fed-batch fermentation processes, when oxygen
603 transfer is not yet limiting. In a recent screening of 52 ascomycete budding yeasts, we noted that *C.*
604 *jadinii* CBS 621 was the fastest-growing strains on a synthetic medium containing ethanol as sole
605 carbon source (11). In the present study, multiple *C. jadinii* strains showed specific growth rates on
606 ethanol close to 0.4 h^{-1} (doubling time 1.7 h) in batch cultures grown on a synthetic medium
607 supplemented with a standard vitamin mixture (Fig 2B, 4C-D). With two exceptions, the investigated
608 *C. jadinii* strains were prototrophic and showed maximum specific growth rates on ethanol in
609 vitamin-free media that were only 10-15% lower than in vitamin-supplemented medium. Use of
610 vitamin-free media offers advantages in terms of cost and simplicity of medium preparation and
611 sterilization and, potentially, reduction of contamination risks (70). Moreover, use of a naturally
612 prototrophic yeast strain precludes the need for extensive metabolic engineering strategies, such
613 as recently applied to *S. cerevisiae* (73), to eliminate full vitamin auxotrophies. The thiamine
614 auxotrophy of our initial model strain *C. jadinii* CBS 621 (Fig 3A-C) could be attributed to absence of
615 a Cj*THI4* gene. Thiamine auxotrophy of this strain may enable use of *THI4* as a selectable marker in
616 ongoing research to make *C. jadinii* fully accessible to Cas9-based genome editing (74).

617 Biomass yields of *C. jadinii* CBS 621 in ethanol-limited chemostat cultures with vitamin
618 supplementation, and of two prototrophic *C. jadinii* strains in vitamin-free media, were among the
619 highest reported for yeasts (11) (Fig 4F). The maximum biomass yield ($Y_{x/s}^{max}$) of *C. jadinii* CBS 621 on

620 ethanol of 0.83 $g_{biomass} \cdot (g_{ethanol})^{-1}$ in vitamin-supplemented, ethanol-limited chemostat cultures even
621 approached the theoretical maximum yield on ethanol of 0.84 $g_{biomass} \cdot (g_{ethanol})^{-1}$(14) for ethanol-
622 limited growth with ammonium as the nitrogen source. A previous study on strain CBS 621 that was
623 based on measurements at a single dilution rate (0.10 h^{-1}) reported lower biomass yields than
624 observed in our study (16). A similarly high biomass yield on ethanol (0.82 $g \cdot g^{-1}$) was reported for
625 batch cultures of the related species *Cyberlindnera saturnus* (10). We consistently measured high
626 biomass yields in replicate cultures of different *C. jadinii* strains, both on vitamin-supplemented and
627 vitamin-free media, checked carbon recoveries of the chemostat cultures and confirmed that no
628 biomass retention occurred (75) and therefore trust our reported data.

629 Ethanol-limited chemostat cultures of *C. jadinii* showed a 25% higher biomass yield on ethanol than
630 cultures of *S. cerevisiae* grown under the same set of conditions (Fig. 1). This difference can be
631 attributed to the presence and absence, respectively, of genes encoding a proton-pumping Complex
632 I NADH dehydrogenase in these two yeasts (11). In contrast to the difference observed in ethanol-
633 limited cultures (14, 16, 76), biomass yields of *C. jadinii* and *S. cerevisiae* in aerobic glucose-limited
634 cultures differed by only 6% (Fig 1). This observation suggests that the contribution of Complex I to
635 respiratory reoxidation of NADH by *C. jadinii* may be carbon-source dependent. A deeper
636 understanding of the role and regulation of Complex I in *C. jadinii* may contribute to improving yields
637 of biomass and other ATP-intensive products, also on carbon- and energy sources other than
638 ethanol. Our current lack of understanding on this subject is illustrated by the observation that,
639 counterintuitively, levels of the non-proton-pumping single-subunit NADH dehydrogenase *Cj*Ndi1
640 were approximately 150-fold higher in the proteome of ethanol-limited cultures of *C. jadinii* than in
641 glucose-limited cultures (Fig S1A, Supp Material S1). Further research should also address the
642 question of how subcellular localization of key enzymes and/or redox shuttle mechanisms enable
643 reoxidation of NADH generated by ethanol and acetaldehyde dehydrogenases, enzymes that can

644 occur in the cytosol as well as in the mitochondrial matrix of yeasts (77) by Complex I, whose
645 catalytic site is in the mitochondrial matrix.

646 The estimated growth-rate independent maintenance energy requirement for ATP (m_{ATP}) of ethanol-
647 limited cultures of *C. jadinii* (2.7 mmol ATP · ($g_{biomass}^{-1}$) · h^{-1}, Fig 2F) was higher than the m_{ATP} of 1.2 mmol
648 ATP · ($g_{biomass}$)$^{-1}$ · h^{-1} estimated from a study on aerobic, glucose-limited chemostat cultures of the
649 Complex-I containing yeast *Komagataella phaffii*, grown at dilution rates ranging from 0.025 to 0.10
650 h^{-1} (78). In energy-substrate-limited cultures, a high maintenance energy requirement most strongly
651 affects biomass yields at low specific growth rates, where it needs a large fraction of the substrate
652 to be respired instead of converted to biomass. Consequently, and consistent with model-based
653 simulations that included the high maintenance requirement of *C. jadinii*, high-cell-density fed-
654 batch cultures did not attain the biomass yields reached in ethanol-limited chemostat cultures
655 grown at intermediate rates (Fig 3C, 4F, 5H) . Protein turnover has been reported to account for a
656 large share of the ATP requirement for cellular maintenance in *S. cerevisiae* (79). Interestingly, two
657 heterologous-protein producing *K. phaffii* strains were reported to exhibit 2-fold higher maintenance-
658 energy requirements than a reference strain (78, 80). This raises the question of whether the high
659 m_{ATP} of *C. jadinii* may be related to its high protein content, and particularly the remarkably high levels
660 of specific proteins involved in ethanol metabolism.

661 Under substrate-limited conditions, competitiveness of micro-organisms is determined by their
662 affinity for the growth-limiting substrate, i.e. the ability to sustain a high biomass-specific
663 consumption rate (q_s) at a low concentration (c_s) of that substrate. Based on the Monod equation (q_s
664 $= q_{s,max} (c_s/(c_s + k_s))$), affinity can be defined as $q_{s,max}/K_S$ (81), in which $q_{s,max}$ is the maximum biomass-
665 specific substrate uptake rate and K_s is the value of c_s at which $q_s = ½ \cdot q_{s,max}$. At low specific growth
666 rates, a large fraction of the proteome of ethanol-limited cultures of *C. jadinii* was allocated to
667 enzymes that catalyse the first three reactions of ethanol metabolism (Fig 2I) and, in particular, to

668 alcohol dehydrogenase (Fig 2J). This observation indicates that, at low specific growth rates, *C.*
669 *jadinii* increases its affinity for ethanol by increasing $q_{s,max}$. This adaptation strategy resembles
670 regulation of methanol oxidase, the first enzyme in methanol metabolism, in *Ogataea polymorpha*.
671 In slow-growing (0.03 h^{-1}) methanol-limited cultures of this methylotrophic yeast, 20% of its
672 proteome consisted of methanol oxidase (82), which closely resembles the 17% contribution of
673 alcohol-dehydrogenases in ethanol-limited *C. jadinii* cultures grown at 0.025 h^{-1}. We hypothesize
674 that this '$q_{s,max}$ adaptation' to ethanol-limited growth contributes to the observation that, despite
675 lower rates of assimilation and dissimilation at low specific growth rates, *C. jadinii* exhibited an
676 essential growth-rate independent protein content of ca. 54% in ethanol-limited chemostat
677 cultures.

678 Based on the quantitative data obtained from chemostat experiments, we designed a feed profile for
679 high-cell density ethanol-limited fed-batch cultures. A previous study also described based fed-
680 batch cultivation of *C. jadinii* on ethanol, but applied discontinuous ethanol feeding and reached a
681 maximum biomass concentration of 15 $g \cdot (kg_{broth})^{-1}$ (83). By controlled feeding of pure ethanol, which
682 eliminated the need for sterilisation of the feed line, the fed-batch cultures reached 100
683 $g_{biomass} \cdot (kg_{broth})^{-1}$ in 48 h of cultivation (Fig 5D). Experimental data on biomass formation were in
684 excellent agreement with model predictions. However, the protein content of biomass harvested at
685 the end of high-cell density fed-batch cultures, when the specific growth rate had decreased to 0.02
686 h^{-1}, had decreased to only 42%. Further research is needed to assess whether this marked difference
687 with the protein content in slow-growing chemostat cultures is due to the dynamic growth-rate
688 profile in the fed-batch cultures, imperfect mixing of the pure ethanol feed, or other factors.

689 **Conclusions**

690 Based on different analyses on ethanol-grown batch, chemostat and fed-batch cultures, the present
691 study provides a quantitative physiology baseline for fundamental and applied research on *C. jadinii*.
692 Its high maximum growth rate, high energetic efficiency of ethanol dissimilation, simple nutritional
693 requirements and high protein content, make this yeast a highly interesting platform for production
694 of SCP and other products from ethanol produced by low-emission technologies. Especially for SCP
695 applications, an observed difference in protein content between ethanol chemostat and fed-batch
696 cultures that were grown over the same range of specific growth rates, merits further investigation.
697 From a fundamental science perspective, our results identify questions about regulation, energy
698 coupling and compartmentation of NADH reoxidation during growth of yeasts and fungi during
699 growth on non-conventional substrates. In addition, the results underline the key role of
700 maintenance energy requirements in high-cell-density fed-batch processes.

701 **Declarations**

702 **Ethics approval and consent to participate**

703 Not applicable

704 **Consent for publication**

705 Not applicable

706 **Availability of data and materials**

707 All data generated or analysed during this study are included in this published article and its
708 supplementary information files.

709 **Competing interests**

710 The company dsm-firmenich owns intellectual property rights of technology discussed in this paper.
711 MAVL and JTP are co-inventors on patent applications related to the present work.

712 **Funding**

713 Co-funding was obtained from dsm-firmenich and from a supplementary grant 'TKI- Toeslag' for
714 Topconsortia for Knowledge and Innovation (TKI's) of the Netherlands Ministry of Economic Affairs
715 and Climate Policy (CHEMIE.PGT.2021.003). The PhD project of MW is funded from a Stevin Prize
716 awarded to JTP by the Dutch Research Council (NWO).

717 **Authors' contributions**

718 MAVL: investigation, methodology, analysis, data visualization, writing (original draft, reviewing and
719 editing). MW: investigation, methodology, analysis, writing (reviewing and editing). EdH and MvdB:
720 investigation, methodology. JMD: conceptualization, writing (reviewing and editing). JTP:
721 conceptualization, supervision, writing (reviewing and editing).

722 **Acknowledgements**

723 The authors thank Clara Carqueija Cardoso for the help with DNA sequencing, Christiaan Mooiman
724 for assistance with the fed-batch experiments, Marijke Luttik for the help with growth experiments,
725 Chris Klomp and Niels Tiemersma for evaluating the methods for biomass composition and help with
726 bioreactor cultivation, and Jordy Elfering for the testing of the serial dilution method and screening
727 and for help with bioreactor cultivation. We thank André Vente for the amino acid and proteome
728 analyses, and Mickel Jansen and Tjeerd van Rij for the input in the project.

729 **References**

730 1. Claassens NJ, Cotton CAR, Kopljar D, Bar-Even A. Making quantitative sense of
731 electromicrobial production. Nature Catalysis. 2019;2(5):437-47.

732 2. Leger D, Matassa S, Noor E, Shepon A, Milo R, Bar-Even A. Photovoltaic-driven microbial
733 protein production can use land and sunlight more efficiently than conventional crops. Proc Natl
734 Acad Sci U S A. 2021;118(26).
735 3. Lynd LR, Beckham GT, Guss AM, Jayakody LN, Karp EM, Maranas C, et al. Toward low-cost
736 biological and hybrid biological/catalytic conversion of cellulosic biomass to fuels. Energy &
737 Environmental Science. 2022;15(3):938-90.
738 4. Martin ME, Richter H, Saha S, Angenent LT. Traits of selected *Clostridium* strains for syngas
739 fermentation to ethanol. Biotechnol Bioeng. 2016;113(3):531-9.
740 5. Smith WA, Burdyny T, Vermaas DA, Geerlings H. Pathways to Industrial-Scale Fuel Out of
741 Thin Air from CO2 Electrolysis. Joule. 2019;3(8):1822-34.
742 6. Christodoulou X, Okoroafor T, Parry S, Velasquez-Orta SB. The use of carbon dioxide in
743 microbial electrosynthesis: Advancements, sustainability and economic feasibility. Journal of CO2
744 Utilization. 2017;18:390-9.
745 7. Cabau-Peinado O, Winkelhorst M, Stroek R, de Kat Angelino R, Straathof AJJ, Masania K, et
746 al. Microbial electrosynthesis from CO_2 reaches productivity of syngas and chain elongation
747 fermentations. Trends Biotechnol. 2024.
748 8. Jansen MLA, Bracher JM, Papapetridis I, Verhoeven MD, de Bruijn H, de Waal PP, et al.
749 *Saccharomyces cerevisiae* strains for second-generation ethanol production: from academic
750 exploration to industrial implementation. FEMS Yeast Res. 2017;17(5).
751 9. Takors R, Kopf M, Mampel J, Bluemke W, Blombach B, Eikmanns B, et al. Using gas mixtures
752 of CO, CO_2 and H_2 as microbial substrates: the do's and don'ts of successful technology transfer
753 from laboratory to production scale. Microb Biotechnol. 2018;11(4):606-25.

754 10. Van Peteghem L, Sakarika M, Matassa S, Rabaey K. The Role of Microorganisms and Carbon-
755 to-Nitrogen Ratios for Microbial Protein Production from Bioethanol. Appl Environ Microbiol.
756 2022;88(22):e0118822.
757 11. Warmerdam M, Vieira-Lara MA, Mans R, Daran JM, Pronk JT. Specific growth rates and growth
758 stoichiometries of Saccharomycotina yeasts on ethanol as sole carbon and energy substrate.
759 Manuscript in preparation. 2024.
760 12. Kotyk A, Alonso A. Transport of ethanol in baker's yeast. Folia Microbiol (Praha).
761 1985;30(1):90-1.
762 13. Kozak BU, van Rossum HM, Niemeijer MS, van Dijk M, Benjamin K, Wu L, et al. Replacement
763 of the initial steps of ethanol metabolism in *Saccharomyces cerevisiae* by ATP-independent
764 acetylating acetaldehyde dehydrogenase. FEMS Yeast Res. 2016;16(2):fow006.
765 14. Verduyn C, Stouthamer AH, Scheffers WA, van Dijken JP. A theoretical evaluation of growth
766 yields of yeasts. Antonie Van Leeuwenhoek. 1991;59(1):49-63.
767 15. Juergens H, Hakkaart XDV, Bras JE, Vente A, Wu L, Benjamin KR, et al. Contribution of
768 Complex I NADH Dehydrogenase to Respiratory Energy Coupling in Glucose-Grown Cultures of
769 *Ogataea parapolymorpha*. Appl Environ Microbiol. 2020;86(15).
770 16. Verduyn C. Physiology of yeasts in relation to biomass yields. Antonie Van Leeuwenhoek.
771 1991;60(3-4):325-53.
772 17. Joseph-Horne T, Hollomon DW, Wood PM. Fungal respiration: a fusion of standard and
773 alternative components. Biochim Biophys Acta. 2001;1504(2-3):179-95.
774 18. Nosek J, Fukuhara H. NADH dehydrogenase subunit genes in the mitochondrial DNA of
775 yeasts. J Bacteriol. 1994;176(18):5622-30.
776 19. Sousa-Silva M, Vieira D, Soares P, Casal M, Soares-Silva I. Expanding the Knowledge on the
777 Skillful Yeast *Cyberlindnera jadinii*. J Fungi (Basel). 2021;7(1).

778 20. Averet N, Jobin ML, Devin A, Rigoulet M. Proton pumping complex I increases growth yield in
779 *Candida utilis*. Biochim Biophys Acta. 2015;1847(10):1320-6.
780 21. Rupp O, Brinkrolf K, Buerth C, Kunigo M, Schneider J, Jaenicke S, et al. The structure of the
781 *Cyberlindnera jadinii* genome and its relation to *Candida utilis* analyzed by the occurrence of single
782 nucleotide polymorphisms. J Biotechnol. 2015;211:20-30.
783 22. Solomons G, Litchfield JH. Single cell protein. Critical Reviews in Biotechnology.
784 1983;1(1):21-58.
785 23. Lallemand. Exploring Lallemand's Torula Yeast: A Remarkable Journey [Available from:
786 https://bio-lallemand.com/savory-ingredients/exploring-lallemands-torula-yeast-specialties/.
787 24. Agboola JO, Lapeña D, Øverland M, Arntzen MØ, Mydland LT, Hansen JØ. Yeast as a novel
788 protein source - Effect of species and autolysis on protein and amino acid digestibility in Atlantic
789 salmon (Salmo salar). Aquaculture. 2022;546.
790 25. Cruz A, Sterten H, Steinhoff FS, Mydland LT, Overland M. *Cyberlindnera jadinii* yeast as a
791 protein source for broiler chickens: effects on growth performance and digestive function from
792 hatching to 30 days of age. Poult Sci. 2020;99(6):3168-78.
793 26. Cruz A, Tauson A-H, Matthiesen CF, Mydland LT, Øverland M. *Cyberlindnera jadinii* yeast as
794 a protein source for growing pigs: Effects on protein and energy metabolism. Livestock Science.
795 2020b;231.
796 27. Burkholder PR, McVeigh I, Moyer D. Studies on some growth factors of yeasts. Journal of
797 Bacteriology. 1944;48(4):385-91.
798 28. Jones SW, Karpol A, Friedman S, Maru BT, Tracy BP. Recent advances in single cell protein
799 use as a feed ingredient in aquaculture. Curr Opin Biotechnol. 2020;61:189-97.
800 29. Nyyssola A, Suhonen A, Ritala A, Oksman-Caldentey KM. The role of single cell protein in
801 cellular agriculture. Curr Opin Biotechnol. 2022;75:102686.

802 30. Ritala A, Hakkinen ST, Toivari M, Wiebe MG. Single Cell Protein-State-of-the-Art, Industrial
803 Landscape and Patents 2001-2016. Front Microbiol. 2017;8:2009.
804 31. Spalvins. Improving single cell protein yields and amino acid profile via mutagenesis: review
805 of applicable amino acid inhibitors for mutant selection. 2021.
806 32. Choi KR, Yu HE, Lee SY. Microbial food: microorganisms repurposed for our food. Microb
807 Biotechnol. 2022;15(1):18-25.
808 33. Hensing MCM, Vrouwenvelder JS, Hellinga C, Van Dijken JP, Pronk JT. Use of chemostat data
809 for modelling extracellular-inulinase production by *Kluyveromyces marxianus* in a high-cell-density
810 fed-batch process. Journal of Fermentation and Bioengineering. 1995;79(1):54-8.
811 34. Verduyn C, Postma E, Scheffers WA, Van Dijken JP. Effect of benzoic acid on metabolic fluxes
812 in yeasts: a continuous-culture study on the regulation of respiration and alcoholic fermentation.
813 Yeast. 1992;8(7):501-17.
814 35. Hazan R, Que YA, Maura D, Rahme LG. A method for high throughput determination of viable
815 bacteria cell counts in 96-well plates. BMC Microbiol. 2012;12:259.
816 36. Lange HC, Heijnen JJ. Statistical reconciliation of the elemental and molecular biomass
817 composition of *Saccharomyces cerevisiae*. Biotechnol Bioeng. 2001;75(3):334-44.
818 37. Pirt SJ. The maintenance energy of bacteria in growing cultures. Proc R Soc Lond B Biol Sci.
819 1965;163(991):224-31.
820 38. van Hoek P, de Hulster E, van Dijken JP, Pronk JT. Fermentative capacity in high-cell-density
821 fed-batch cultures of baker's yeast. Biotechnol Bioeng. 2000;68(5):517-23.
822 39. Puiman L, Elisiário MP, Crasborn LML, Wagenaar LECH, Straathof AJJ, Haringa C. Gas mass
823 transfer in syngas fermentation broths is enhanced by ethanol. Biochemical Engineering Journal.
824 2022;185.

825 40. Garcia-Ochoa F, Gomez E. Bioreactor scale-up and oxygen transfer rate in microbial
826 processes: an overview. Biotechnol Adv. 2009;27(2):153-76.
827 41. Postma E, Verduyn C, Scheffers WA, Van Dijken JP. Enzymic analysis of the crabtree effect in
828 glucose-limited chemostat cultures of *Saccharomyces cerevisiae*. Appl Environ Microbiol.
829 1989;55(2):468-77.
830 42. Mashego MR, van Gulik WM, Vinke JL, Heijnen JJ. Critical evaluation of sampling techniques
831 for residual glucose determination in carbon-limited chemostat culture of *Saccharomyces*
832 *cerevisiae*. Biotechnol Bioeng. 2003;83(4):395-9.
833 43. Guadalupe Medina V, Almering MJ, van Maris AJ, Pronk JT. Elimination of glycerol production
834 in anaerobic cultures of a *Saccharomyces cerevisiae* strain engineered to use acetic acid as an
835 electron acceptor. Appl Environ Microbiol. 2010;76(1):190-5.
836 44. Johnson KR, Ellis G, Toothill C. The sulfophosphovanillin reaction for serum lipids: a
837 reappraisal. Clin Chem. 1977;23(9):1669-78.
838 45. Izard J, Limberger RJ. Rapid screening method for quantitation of bacterial cell lipids from
839 whole cells. J Microbiol Methods. 2003;55(2):411-8.
840 46. Benthin S, Nielsen J, Villadsen J. A simple and reliable method for the determination of
841 cellular RNA content. Biotechnology Techniques. 1991;5(1):39-42.
842 47. Herbert D, Phipps PJ, Strange RE. Chapter III Chemical Analysis of Microbial Cells. Methods
843 in Microbiology1971. p. 209-344.
844 48. Hebert AS, Richards AL, Bailey DJ, Ulbrich A, Coughlin EE, Westphall MS, et al. The one hour
845 yeast proteome. Mol Cell Proteomics. 2014;13(1):339-47.
846 49. Li H, Durbin R. Fast and accurate short read alignment with Burrows-Wheeler transform.
847 Bioinformatics. 2009;25(14):1754-60.

848 50. Li H, Handsaker B, Wysoker A, Fennell T, Ruan J, Homer N, et al. The Sequence
849 Alignment/Map format and SAMtools. Bioinformatics. 2009;25(16):2078-9.
850 51. Walker BJ, Abeel T, Shea T, Priest M, Abouelliel A, Sakthikumar S, et al. Pilon: an integrated
851 tool for comprehensive microbial variant detection and genome assembly improvement. PLoS One.
852 2014;9(11):e112963.
853 52. Wickham H, Wickham H. ggplot2: Springer; 2016.
854 53. Prjibelski A, Antipov D, Meleshko D, Lapidus A, Korobeynikov A. Using SPAdes De Novo
855 Assembler. Curr Protoc Bioinformatics. 2020;70(1):e102.
856 54. Agboola JO, Øverland M, Skrede A, Hansen JØ. Yeast as major protein-rich ingredient in
857 aquafeeds: a review of the implications for aquaculture production. Reviews in Aquaculture.
858 2020;13(2):949-70.
859 55. Wronska AK, Haak MP, Geraats E, Bruins Slot E, van den Broek M, Pronk JT, et al. Exploiting
860 the Diversity of Saccharomycotina Yeasts To Engineer Biotin-Independent Growth of
861 *Saccharomyces cerevisiae*. Appl Environ Microbiol. 2020;86(12):e00270-20.
862 56. van Bodegom P. Microbial maintenance: a critical review on its quantification. Microb Ecol.
863 2007;53(4):513-23.
864 57. Vos T, Hakkaart XD, de Hulster EA, van Maris AJ, Pronk JT, Daran-Lapujade P. Maintenance-
865 energy requirements and robustness of *Saccharomyces cerevisiae* at aerobic near-zero specific
866 growth rates. Microb Cell Fact. 2016;15(1):111.
867 58. Paredes-Lopez O, Camargo-Rubio E, Ornelas-Vale A. Influence of specific growth rate on
868 biomass yield, productivity, and compostion of *Candida utilis* in batch and continuous culture. Appl
869 Environ Microbiol. 1976;31(4):487-91.

870 59. van Winden WA, Mans R, Breestraat S, Verlinden RAJ, Mielgo-Gomez A, de Hulster EAF, et al.
871 Towards closed carbon loop fermentations: Cofeeding of *Yarrowia lipolytica* with glucose and formic
872 acid. Biotechnol Bioeng. 2022;119(8):2142-51.
873 60. Bruinenberg PM, Jonker R, Vandijken JP, Scheffers WA. Utilization of Formate as an
874 Additional Energy-Source by Glucose-Limited Chemostat Cultures of *Candida utilis* CBS 621 and
875 *Saccharomyces cerevisiae* CBS 8066 - Evidence for the Absence of Transhydrogenase Activity in
876 Yeasts. Arch Microbiol. 1985;142(3):302-6.
877 61. Mor JR, Fiechter A. Continuous cultivation of *Saccharomyces cerevisiae*. I. Growth on
878 ethanol under steady-state conditions. Biotechnology and Bioengineering. 1968;10(2):159-76.
879 62. Fonseca GG, Gombert AK, Heinzle E, Wittmann C. Physiology of the yeast *Kluyveromyces*
880 *marxianus* during batch and chemostat cultures with glucose as the sole carbon source. FEMS Yeast
881 Res. 2007;7(3):422-35.
882 63. Waldron C, Lacroute F. Effect of growth rate on the amounts of ribosomal and transfer
883 ribonucleic acids in yeast. J Bacteriol. 1975;122(3):855-65.
884 64. Elsemman IE, Rodriguez Prado A, Grigaitis P, Garcia Albornoz M, Harman V, Holman SW, et
885 al. Whole-cell modeling in yeast predicts compartment-specific proteome constraints that drive
886 metabolic strategies. Nat Commun. 2022;13(1):801.
887 65. Bruggeman FJ, Planque R, Molenaar D, Teusink B. Searching for principles of microbial
888 physiology. FEMS Microbiol Rev. 2020;44(6):821-44.
889 66. Klumpp S, Scott M, Pedersen S, Hwa T. Molecular crowding limits translation and cell growth.
890 Proc Natl Acad Sci U S A. 2013;110(42):16754-9.
891 67. Consortium U. UniProt: a worldwide hub of protein knowledge. Nucleic acids research.
892 2019;47(D1):D506-D15.

893 68. Shen Y, Dinh HV, Cruz E, Call CM, Baron H, Ryseck R-P, et al. Proteome capacity constraints
894 favor respiratory ATP generation. 2022.
895 69. Schomburg I, Jeske L, Ulbrich M, Placzek S, Chang A, Schomburg D. The BRENDA enzyme
896 information system-From a database to an expert system. J Biotechnol. 2017;261:194-206.
897 70. Perli T, Wronska AK, Ortiz-Merino RA, Pronk JT, Daran JM. Vitamin requirements and
898 biosynthesis in *Saccharomyces cerevisiae*. Yeast. 2020;37(4):283-304.
899 71. Yasukawa T, Oda AH, Nakamura T, Masuo N, Tamura M, Yamasaki Y, et al. TAQing2.0 for
900 genome reorganization of asexual industrial yeasts by direct protein transfection. Commun Biol.
901 2022;5(1):144.
902 72. Council NR. Nutrient Requirements of Fish and Shrimp. Washington, DC: The National
903 Academies Press; 2011. 392 p.
904 73. Ehrmann AK, Wronska AK, Perli T, de Hulster EAF, Luttik MAH, van den Broek M, et al.
905 Engineering *Saccharomyces cerevisiae* for fast vitamin-independent aerobic growth. Metab Eng.
906 2024;82:201-15.
907 74. Gu L, Zhang R, Fan X, Wang Y, Ma K, Jiang J, et al. Development of CRISPR/Cas9-Based
908 Genome Editing Tools for Polyploid Yeast *Cyberlindnera jadinii* and Its Application in Engineering
909 Heterologous Steroid-Producing Strains. ACS Synth Biol. 2023;12(10):2947-60.
910 75. Noorman H, Baksteen J, Heijnen J, Luyben CA. The bioreactor overflow device: an undesired
911 selective separator in continuous cultures? Microbiology. 1991;137(9):2171-7.
912 76. van Urk H, Postma E, Scheffers WA, van Dijken JP. Glucose transport in crabtree-positive and
913 crabtree-negative yeasts. J Gen Microbiol. 1989;135(9):2399-406.
914 77. Bakker BM, Bro C, Kotter P, Luttik MA, van Dijken JP, Pronk JT. The mitochondrial alcohol
915 dehydrogenase Adh3p is involved in a redox shuttle in *Saccharomyces cerevisiae*. J Bacteriol.
916 2000;182(17):4730-7.

917 78. Rebnegger C, Vos T, Graf AB, Valli M, Pronk JT, Daran-Lapujade P, et al. *Pichia pastoris*
918 Exhibits High Viability and a Low Maintenance Energy Requirement at Near-Zero Specific Growth
919 Rates. Appl Environ Microbiol. 2016;82(15):4570-83.
920 79. Hong KK, Hou J, Shoaie S, Nielsen J, Bordel S. Dynamic ^{13}C-labeling experiments prove
921 important differences in protein turnover rate between two *Saccharomyces cerevisiae* strains. FEMS
922 Yeast Res. 2012;12(7):741-7.
923 80. Maurer M, Kuhleitner M, Gasser B, Mattanovich D. Versatile modeling and optimization of fed
924 batch processes for the production of secreted heterologous proteins with *Pichia pastoris*. Microb
925 Cell Fact. 2006;5(1):37.
926 81. Button DK. Kinetics of nutrient-limited transport and microbial growth. Microbiol Rev.
927 1985;49(3):270-97.
928 82. van Dijken JP, Otto R, Harder W. Growth of *Hansenula polymorpha* in a methanol-limited
929 chemostat. Physiological responses due to the involvement of methanol oxidase as a key enzyme in
930 methanol metabolism. Arch Microbiol. 1976;111(1-2):137-44.
931 83. Watteeuw CM, Armiger WB, Ristroph DL, Humphrey AE. Production of single cell protein from
932 ethanol by fed-batch process. Biotechnology and Bioengineering. 1979;21(7):1221-37.

933

934

935 **Supplemental Materials**

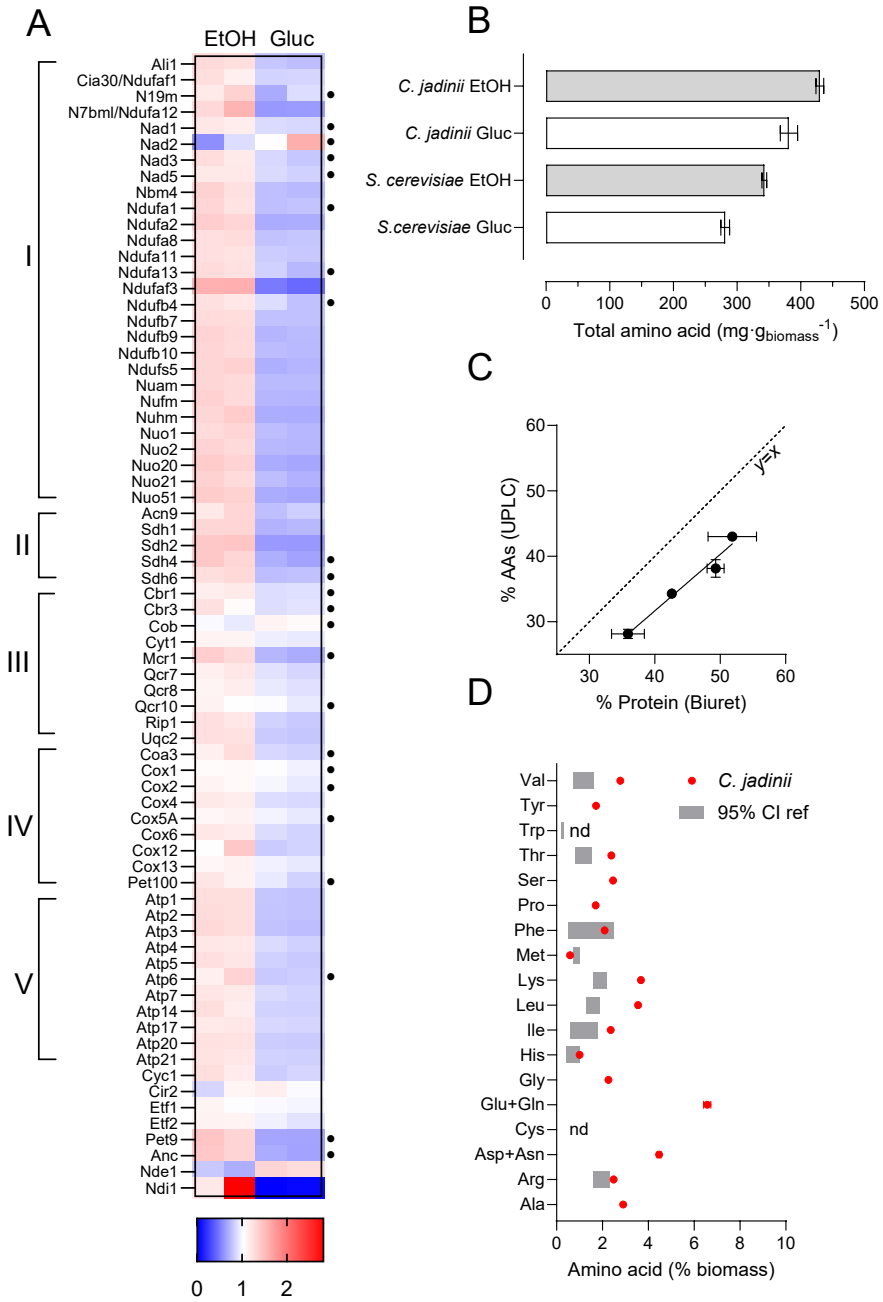

936

937 **Figure S1: Amino acid composition and OXPHOS proteins.** (A) Heatmap of proteins involved in oxidative
938 phosphorylation (OXPHOS) in ethanol- (EtOH) vs glucose-grown (Gluc) *C. jadinii*. Levels were normalized to
939 average levels across all samples. Blue: low levels, red: high levels. Protein names and UniProt ID's are found
940 in Supp. Material S1. Dots next to each row on the right represent predicted membrane proteins. Roman
941 numerals on the left represent respiratory complex (I-IV) and F_1F_o-ATP synthase (V). (B) Total amino acid
942 residue concentration in *S. cerevisiae* and *C. jadinii* grown on glucose or ethanol as substrate in chemostats.

943 (C) Comparison of total amino acid levels (y-axis) and total protein measured with the Biuret method (x-axis).
944 The dashed line is the identity line (y=x). (D) Amino acid levels in ethanol-grown *C. jadinii* (red dots) compared
945 to the 95% confidence interval (CI) of amino acid levels needed for feed formulation in aquaculture (from (72)),
946 grey boxes, n =2.

947

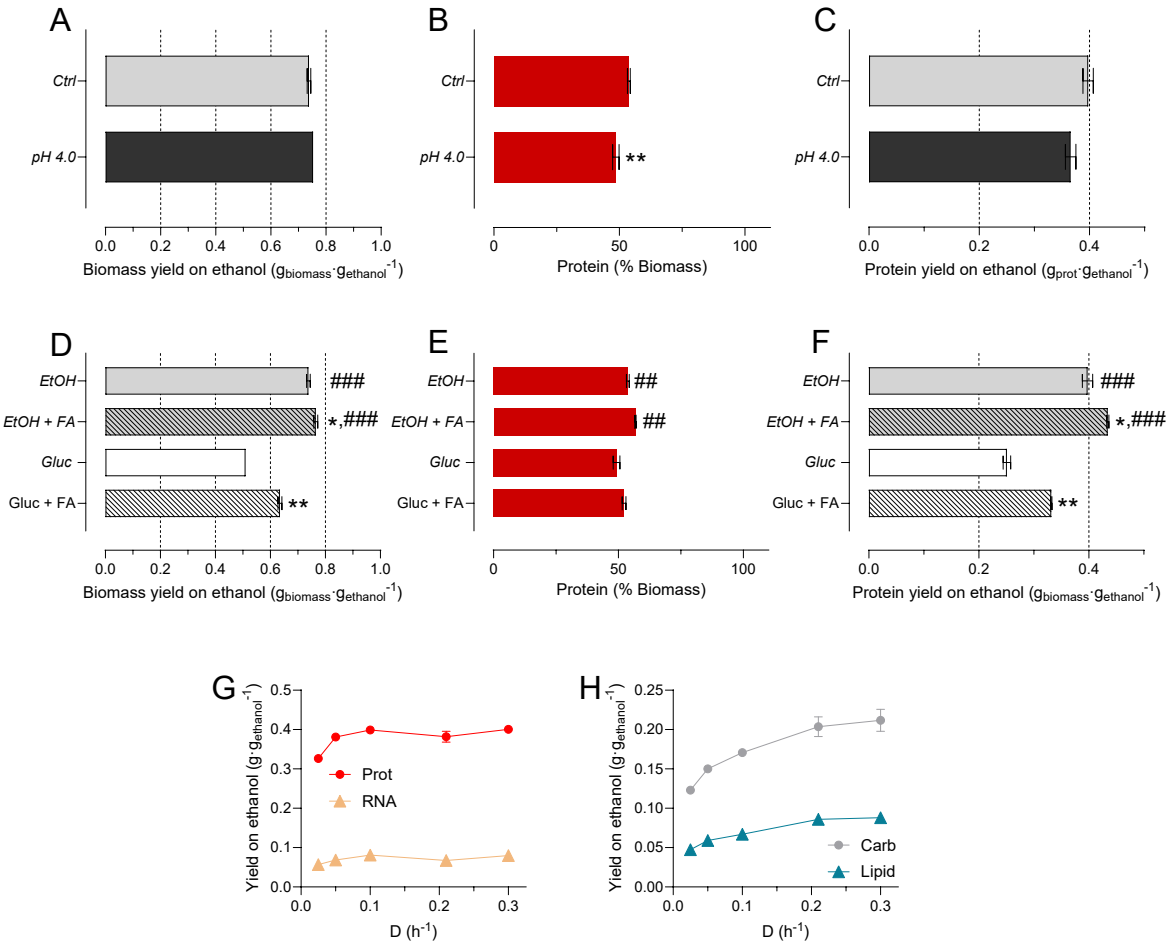

Figure S2: Yields of biomass components and strategies to increase biomass yield (A) Biomass yield on substrate, (B) protein content as a percentage of the biomass and (C) protein yields on substrate for *C. jadinii* grown in ethanol-limited cultures at either pH 5.0 (Ctrl) or pH 4.0. (D) Biomass yield on substrate, (E) protein content as a percentage of the biomass and (F) protein yields on substrate for *C. jadinii* grown in ethanol (EtOH) or glucose-limited (Gluc) chemostats in the presence or absence of formic acid (FA). The ratio of formic acid to substrate was defined as 1.2 Cmol/Cmol: 2.4 mol FA per mol ethanol and 7.2 mol FA per mol glucose. (G) and (H) Yields of the main components of the biomass in $g \cdot g_s^{-1}$: proteins (Prot), RNA, carbohydrates (Carb) and lipids, ##p<0.01 ###p<0.001, ethanol- (EtOH) vs glucose-grown (Gluc). *p<0.05, **p<0.01, effect of either pH or FA addition, n=2.

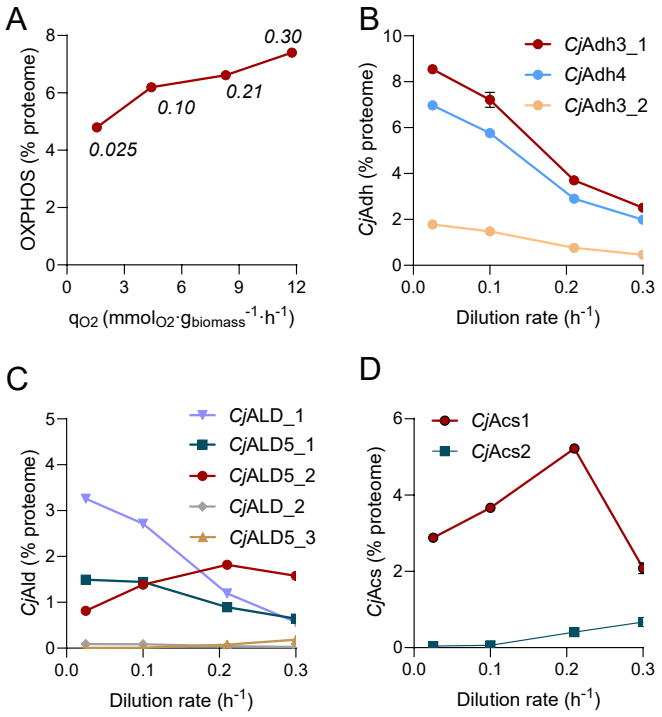

Figure S3: Proteome allocation of OXPHOS and ethanol catabolism proteins. (A) Percentage of the proteome occupied by OXPHOS proteins versus the oxygen consumption rates (q_{O_2}). Indicated in italics are the respective dilution rates. (B) Alcohol dehydrogenase (*Cj*Adh) isoforms, (B) aldehyde dehydrogenase isoforms (*Cj*Ald) and (C) acetyl-CoA synthetase isoforms (*Cj*Acs) as a function of the dilution rate. Protein names and UniProt ID's are found in Supp. Material S2, n =2.

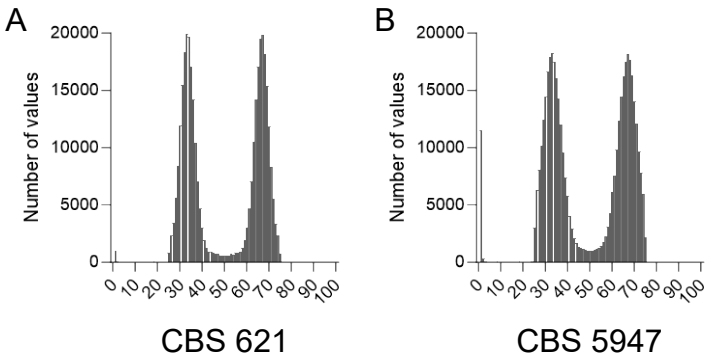

Figure S4: SNP distribution. Reads were mapped to the haploid consensus genome. SNPs were detected and the percentage of reads (vs total reads) for each SNP were computed and plotted as histograms. The peaks at around 33% and 66% show that SNPs occupy either 1/3 or 2/3 of each location, indicating that (A) CBS 621 and (B) CBS 5947 are triploid strains.

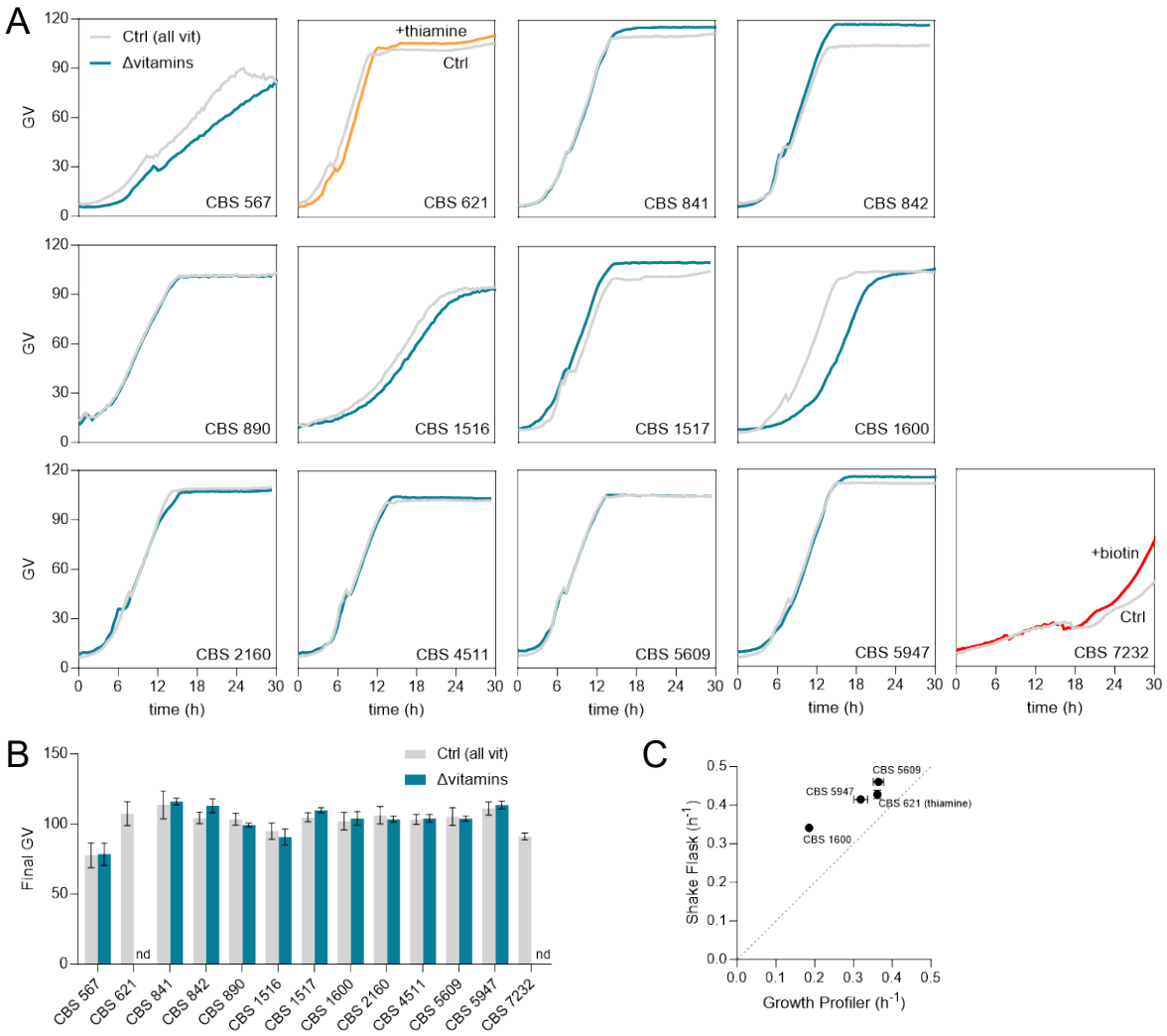

Figure S5: Growth curves of 13 *C. jadinii* strains. (A) Representative traces of individual growth curves for all tested strains. Traces represent cultures grown at dilution 1×, $OD_{initial}$ = 0.2. Grey lines represent the control (with added vitamins), blue lines represent cultures grown in the absence of added vitamins. For CBS 621 and CBS 7232, which do not grow in the absence of all vitamins, thiamine and biotin were added as sole vitamins, respectively. (B) Final green values (GV) at the stationary phase for all conditions, nd: non-detectable. (C) Correlation of the growth rates obtained in the Growth Profiler (x-axis) with those obtained in shake flasks (y-axis) for strains grown in the absence of vitamins, n=2-3.

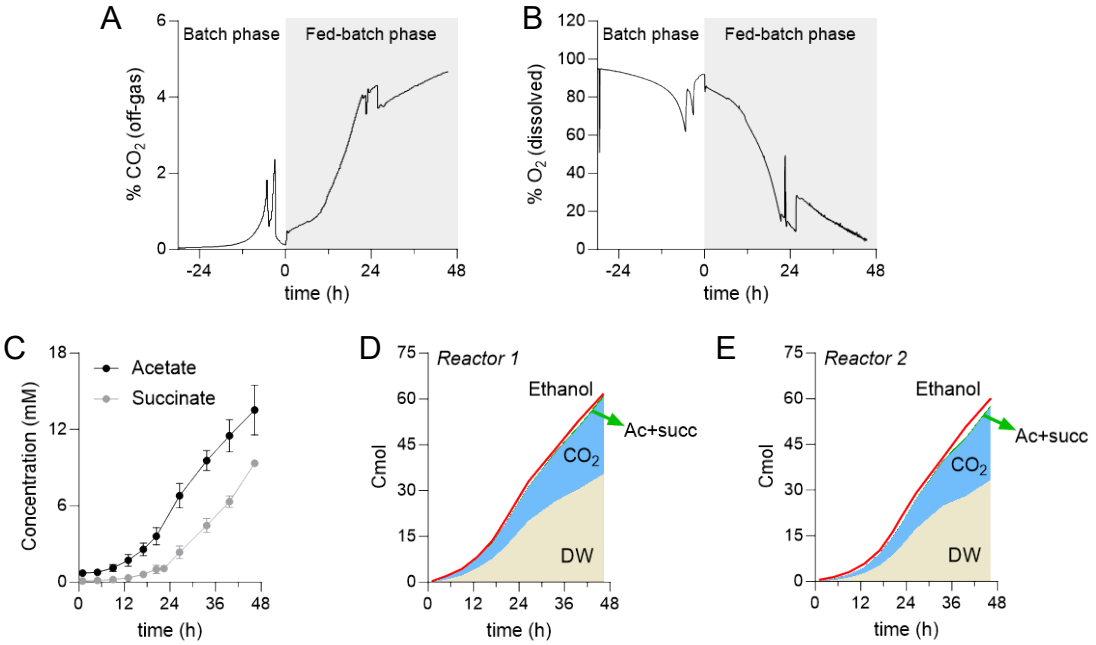

Figure S6: Fed-batch representative traces and carbon recovery. (A) Representative CO_2 concentration in the off-gas and (B) dissolved oxygen (DO) concentration, both during batch and fed-batch phases for reactor 2. (C) Acetate and succinate concentrations in the residuals during the fed-batch phase. (D-E) carbon balance time course for reactors 1 and 2, respectively. The red line represents the total amount of ethanol consumed. The shaded areas correspond to biomass (DW), CO_2 and organic acids (Ac + succ). All amounts are expressed in Cmol, n=2.

994 **Supplemental Tables**

995 **Table S1: *C. jadinii* and *S. cerevisiae* in glucose- and ethanol-limited growth at 0.10 h^{-1}**
996 **(mean ± SD)**

Strain	Substrate	$Y_{X/S}$ ($g_{biomass} \cdot g_s^{-1}$)	$q_{ethanol}$ ($mmol \cdot g_{biomass}^{-1} \cdot h^{-1}$)	q_{CO_2} ($mmol \cdot g_{biomass}^{-1} \cdot h^{-1}$)	q_{O_2} ($mmol \cdot g_{biomass}^{-1} \cdot h^{-1}$)	RQ
S. cerevisiae	Glucose	0.48 ± 0.00	1.27 ± 0.00	3.31 ± 0.25	2.78 ± 0.13	1.19 ± 0.03
S. cerevisiae	Ethanol	0.59 ± 0.01	3.64 ± 0.20	3.56 ± 0.10	6.62 ± 0.17	0.54 ± 0.00
C. jadinii	Glucose	0.51 ± 0.01	1.08 ± 0.01	2.99 ± 0.08	2.51 ± 0.12	1.19 ± 0.03
C. jadinii	Ethanol	0.74 ± 0.01	2.87 ± 0.02	2.19 ± 0.02	4.41 ± 0.05	0.50 ± 0.00

997

998 **Table S2: Amino acid composition of the biomass of *C. jadinii* and *S. cerevisiae* in**
999 **glucose- and ethanol-limited growth at 0.10 h^{-1} (mean ± SD). Values are in $mg \cdot g_{biomass}^{-1}$.**

	S. cerevisiae		***C. jadinii***	
Amino acid	**Glucose**	**Ethanol**	**Glucose**	**Ethanol**
Alanine	17.7 ± 0.5	21.4 ± 0.3	25.0 ± 0.8	29.1 ± 0.4
Arginine	15.5 ± 0.4	19.5 ± 0.3	21.2 ± 0.6	24.9 ± 0.3
Aspartate/Asparagine	32.9 ± 0.8	37.8 ± 0.1	40.5 ± 1.3	44.7 ± 0.8
Glutamate/Glutamine	38.2 ± 0.9	60.5 ± 0.6	62.0 ± 2.8	65.7 ± 1.6
Glycine	13.8 ± 0.3	16.7 ± 0.0	19.6 ± 0.6	22.6 ± 0.1
Histidine	6.5 ± 0.2	8.1 ± 0.1	8.2 ± 0.3	10.0 ± 0.1
Isoleucine	15.8 ± 0.4	18.1 ± 0.1	20.4 ± 0.7	23.6 ± 0.1
Leucine	24.0 ± 0.6	27.8 ± 0.4	31.4 ± 1.0	35.5 ± 0.4
Lysine	25.8 ± 0.6	28.7 ± 0.3	31.9 ± 1.2	36.8 ± 0.4
Methionine	5.1 ± 0.1	5.9 ± 0.2	5.2 ± 0.2	5.9 ± 0.1
Phenylalanine	14.5 ± 0.4	16.4 ± 0.2	18.8 ± 0.6	21.0 ± 0.2
Proline	11.8 ± 0.3	13.8 ± 0.0	15.0 ± 0.4	17.1 ± 0.4
Serine	15.7 ± 0.4	17.9 ± 0.4	22.2 ± 1.0	24.6 ± 0.4
Threonine	16.0 ± 0.4	18.2 ± 0.2	21.7 ± 0.8	23.9 ± 0.4
Tyrosine	11.0 ± 0.3	12.7 ± 0.1	14.9 ± 0.2	17.2 ± 0.3
Valine	17.5 ± 0.5	19.6 ± 0.3	23.9 ± 0.8	27.8 ± 0.2

1000

1001 **Table S3: effect of growth rate on ethanol-limited CBS 621 physiology**

Dilution rate (h^{-1})	$Y_{X/S}$ ($g_{biomass} \cdot g_{ethanol}^{-1}$)	$q_{ethanol}$ ($mmol \cdot g_{biomass}^{-1} \cdot h^{-1}$)	q_{CO_2} ($mmol \cdot g_{biomass}^{-1} \cdot h^{-1}$)	q_{O_2} ($mmol \cdot g_{biomass}^{-1} \cdot h^{-1}$)	RQ
0.025 ± 0.00	0.59 ± 0.00	0.93 ± 0.02	0.98 ± 0.03	1.56 ± 0.00	0.63 ± 0.02
0.05 ± 0.00	0.70 ± 0.01	1.54 ± 0.00	1.39 ± 0.01	2.65 ± 0.11	0.52 ± 0.00
0.10 ± 0.00	0.74 ± 0.01	2.87 ± 0.02	2.19 ± 0.02	4.41 ± 0.05	0.50 ± 0.00
0.21 ± 0.00	0.77 ± 0.01	5.90 ± 0.01	3.63 ± 0.02	8.30 ± 0.02	0.44 ± 0.00
0.24 ± 0.00	0.78 ± 0.01	6.69 ± 0.01	3.86 ± 0.04	9.72 ± 0.25	0.40 ± 0.01
0.30 ± 0.00	0.81 ± 0.00	8.18 ± 0.08	4.78 ± 0.11	11.76 ± 0.07	0.41 ± 0.00

1002

1003 **Table S4: Genome sequence of CBS 621 and CBS 5947**

Components	NBRC 0988 (CBS 5609)	NBRC 0988 (CBS 5609)	CBS 621	CBS 5947
NCBI assembly reference	GCA_000328385.1 (2016)	GCA_024346625.1 (2022)		
Assembly level	Chromosomes	Chromosomes	-	-
Genome size	14.3 Mb	13.1 Mb	17.9 Mb	14.7 Mb
Genes	8,864	-	10,949	
No of scaffolds	1,002	7	-	-
Scaffolds N50	189,765	2,424,584	-	-
No of contigs	1,163	7	7,832	6,831
Contigs N50	158,681	2,424,584	3,994	3,299
No of chromosomes	13	6 (+ mtDNA)	-	-
GC-content	44.7	44.5	44.5	44.3
Total of CDS	8,646	-		

1004

1005 **Table S5: Vitamin-dependent physiology of *C. jadinii* strains on ethanol-limited growth**
1006 **at 0.10 h^{-1}**

Strain	Condition	$Y_{X/S}$ ($g_{biomass} \cdot g_{ethanol}^{-1}$)	$q_{ethanol}$ ($mmol \cdot g_{biomass}^{-1} \cdot h^{-1}$)	q_{CO_2} ($mmol \cdot g_{biomass}^{-1} \cdot h^{-1}$)	q_{O_2} ($mmol \cdot g_{biomass}^{-1} \cdot h^{-1}$)	RQ
CBS 621	Ctrl (all vit)	0.74 ± 0.01	2.90 ± 0.02	2.19 ± 0.02	4.40 ± 0.05	0.50 ± 0.00
CBS 1600	Ctrl (all vit)	0.73 ± 0.01	2.94 ± 0.05	2.19 ± 0.04	4.41 ± 0.12	0.50 ± 0.00
CBS 1600	Δ vitamins	0.72 ± 0.01	2.96 ± 0.00	2.25 ± 0.01	4.51 ± 0.01	0.50 ± 0.00
CBS 5609	Δ vitamins	0.70 ± 0.00	3.14 ± 0.16	2.42 ± 0.10	4.99 ± 0.23	0.48 ± 0.00
CBS 5947	Δ vitamins	0.74 ± 0.01	2.95 ± 0.03	2.23 ± 0.05	4.61 ± 0.09	0.48 ± 0.00

1007

1008 **Table S6: Vitamin levels in C. jadinii CBS 5947 at the end of fed-batch and their**
1009 **requirements in aquaculture (DOI: 10.17226/13039)**

Vitamin	Content* ($mg \cdot (kg_{biomass})^{-1}$)	Aquaculture# ($mg \cdot (kg_{diet})^{-1}$)
Thiamine	1.7 ± 0.3	5 ± 2
Riboflavin	15 ± 3	7 ± 1
Niacin	290 ± 140	30 ± 15
Pyridoxine	53 ± 9	7 ± 1

1010 *mean ± SD, #mean ± SEM
1011

Supplemental Materials

Supplemental Material S1: Proteomics dataset *S. cerevisiae* and *C. jadinii* (xlsx)

Supplemental Material S2: Proteomics dataset *C. jadinii* dilution rates (xlsx)

Supplemental Material S3: Derivation of growth rates from serial dilution method

The Growth Profiler is an equipment used for high throughput screening for growth of strains and medium conditions. However, it produces Green Values (GV), which are based on pictures taken from the bottom of the wells. The value of GV is proportional to OD, but not linearly (Fig. S7). To avoid the need of creating an GV to OD calibration curve for each strain tested, we propose a method to derive maximal growth rates (μ_{max}) based on serial sample dilutions, inspired by the method described by (35).

The method is based on serial dilutions of a culture sample to determine its μmax in given conditions. First, a GV in the early exponential phase for each growth curve is selected, namely GV_{select}. In the current manuscript, GV_{select} of 20 was chosen, which will always refer to the same OD for the same species and conditions, given that OD is a function of GV (Fig S7). The time required to reach this specific GV_{select} is recorded for each dilution ($t_{dilution}$). By plotting $t_{dilution}$ (x-axis) against the natural logarithm of the dilution factor (y-axis), one can obtain the μ_{max} as the slope of the fitted line. The mathematical reasoning behind this is addressed below.

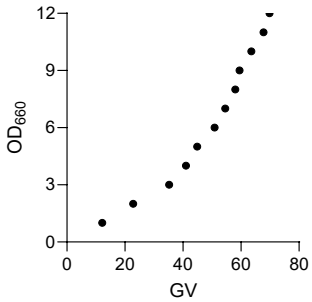

Figure S7: GV to OD conversion curve, obtained for exponentially-growing CBS 621.

The general formula for exponential growth at constant volume is:

$c_t = c_0 \cdot e^{\mu \cdot t}$ (S1)

In which c_t is the cell concentration at elapsed time, c_0 is the starting concentration, μ is the specific growth rate, and t is the elapsed time. Let us consider two cultures of the same species, one inoculated at concentration c_n and other inoculated at concentration c_p, where n and p are the dilution factors in respect to c_0, n>p. After a timespan of t_n and t_p, respectively, they reach a predetermined concentration c_t. Therefore, we can write:

$c_n \cdot e^{\mu \cdot t_n} = c_p \cdot e^{\mu \cdot t_p}$ (S2)

$c_p = c_n \cdot \frac{n}{p}$ (S3)

By substituting c_p in equation S2 according to S3, we have:

$e^{\mu \cdot t_n} = \frac{n}{p} \cdot \ e^{\mu \cdot t_p}$ (S4)

Solving this equation for μ, we have:

$\mu = \frac{\ln n - \ln p}{(t_n - t_p)}$ (S5)

If cells are growing at a $\mu = \mu_{max}$, this can then be rewritten as:

$\mu_{max} = \frac{\ln n - \ln p}{(t_n - t_p)}$ (S6)

Fig. S8A represents the growth curves (in GV) of a specific strain/condition inoculated at dilutions n and p and the GV_{select}. Fig S8B shows a line where the natural logarithms of dilutions (y-axis) are plotted against the time to reach GV_{select} (x-axis). The slope of the curve is equal to equation S6, therefore justifying the validity of the serial dilution method to infer growth rates. This method, however, assumes that no lag phase is present when diluting the samples.

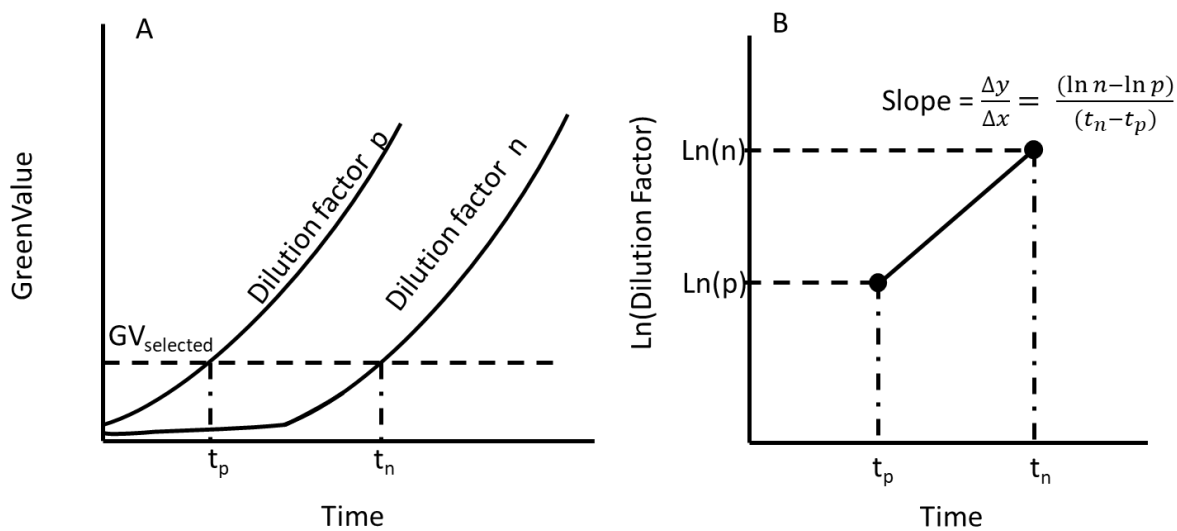

Fig S8: Schematic graphs of the serial dilution method. (A) Growth curves of cultures inoculated at dilution factors p and n, in Green Value against time. Time points t_p and t_n stand for the time when GV_{select} is reached. (B) Natural logarithm of dilution factors p and n plotted against the respective time points t_p and t_n, displayed with the mathematical formula for the slope.